NATIONAL ADVISORY COMMITTEE FOR AERONAUTICS

TECHNICAL NOTE 3043

APPLICATION OF SILVER CHLORIDE IN INVESTIGATIONS OF ELASTO-PLASTIC STATES OF STRESS

By L. E. Goodman and J. G. Sutherland

University of Illinois

Washington
November 1953

NATIONAL ADVISORY COMMITTEE FOR AERONAUT.

TECHNICAL NOTE 3043

APPLICATION OF SILVER CHLORIDE IN INVESTIGATIONS OF ELASTO-PLASTIC STATES OF STRESS

By L. E. Goodman and J. G. Sutherland

SUMMARY

The use of silver chloride as a material for photoelastic stress analysis offers the possibilities of studying both elastic and plastic states of stress in a crystalline metallike material on either a microscale or macroscale. In order to realize this possibility, however, it is first necessary to relate the stress state quantitatively with the observed relative retardation and extinction angle. In this report these relationships are developed from a general theory of stress birefringence, according to a stress-dependent hypothesis. This hypothesis and the resulting analytical relationships have been experimentally vindicated by measurements made on a variety of single-crystal specimens of silver chloride tested in simple tension in the elastic and plastic stress ranges.

With an understanding of the relationship between the stress state and the resulting optical effects, it has been feasible to proceed with studies of relatively complicated stress states. The present work has included a study of the stress states in bicrystal tension specimens, in simple polycrystalline tension specimens, and in single-crystal and polycrystal tension specimens having a hole on the specimen axis. These tests, which are discussed in detail in the body of the report, have yielded qualitative and quantitative information on the elasto-plastic state of stress. Silver chloride appears to be a suitable medium for photoelastic studies of the effect of plastic yielding on the state of stress in a crystalline metallike material.

INTRODUCTION

To a greater or lesser extent, most transparent materials become doubly refracting when subjected to load. This property is the basis of the photoelastic technique in conventional applications of which a model cut from a plate of glass or plastic is loaded and then examined

in polarized light. Under these circumstances the directions of polarization of the rays which have passed through the specimen coincide with the directions of principal stress in the plane perpendicular to the wave normal and the relative phase retardation is proportional to the difference between the principal stresses. Since it provides an accurate quantitative determination of two-dimensional stress states, the photoelastic technique has come to have a recognized place in engineering stress analysis. It has been particularly successful, for example, in the determination of stress concentration factors for shapes too complicated to be amenable to the mathematical theory of elasticity. But its usefulness has, in general, been limited to cases in which perfect elasticity may be assumed. Many of the glasses and plastics conventionally employed are brittle at room temperature. Fried (refs. 1 and 2) has investigated a variety of materials with special reference to cellulose nitrate. Hetényi (ref. 3) has reported a particular long-chain polymer. With the exception of silver chloride, these previously studied materials differ fundamentally from structural metals. They are visco-elastic and amorphous. While the behavior of visco-elastic materials is an important field of study, it should be recognized that structural metals are aggregates of crystals. Their inelastic behavior depends upon the way in which slip occurs in the crystal lattice, upon the redistribution of stress which occurs after a grain has yielded, and upon grain-boundary phenomena.

Silver chloride is an elasto-plastic crystalline material with many of the properties of metals of structural importance (ref. 4). In particular, its behavior at room temperature is elastic at low stress levels, becoming ductile as the stress is raised. It exhibits strain-hardening in the ductile range. In addition, silver chloride is transparent and, being a cubic crystal, it is optically isotropic in the unstressed state. When loaded it becomes doubly refracting so that its effect on polarized light, properly interpreted, can be used to measure the state of stress.

The metallike properties of silver chloride appear first to have been noted by Tammann (ref. 5) in 1932. Stepanov and colleagues in the U.S.S.R. independently recognized the significance of the ductility of silver chloride as early as 1934 (ref. 6). Moeller and others, in a survey of the literature, report that its metallurgical properties have been studied in Italy by Cagliotti and by Levi and Tabet. The feasibility of rolling thin sheets, of extruding tubing, and of pouring ingots of this material was first reported by Fugassi and McKinney (ref. 7) and by Fetters and Dienes (ref. 8) in this country. Probably the most significant uses of the photoelastic properties of silver chloride have been reported by Orowan (ref. 9) and Nye (ref. 10) at the Cavendish Laboratory. West and Makas (ref. 11) have measured the stress-optical constants of silver chloride in the elastic range. Fried (refs. 1 and 2) has commented upon the macroscopic stress-optical properties of

silver chloride in the plastic range. Stepanov (ref. 12) and Prigorovskii (ref. 13) have described the suitability of silver chloride as an optically active medium for the investigation of plastic states of stress.

The present work has first been directed toward providing a quantitative relationship between the quantities which can be observed in the laboratory (relative retardation Δ and extinction angle φ are the ones most easily measured) and the state of elastic or plastic stress in a specimen. Since crystalline silver chloride is photoelastically anisotropic, the directions of polarization of rays which have passed through a specimen do not correspond, in general, to the directions of principal stress. The angles between these two sets of directions depend on the relative magnitudes of the principal stresses and on the relative directions of the incident wave normal, the crystal axes, and the stress axes. The retardation of the transmitted light also depends on these quantities. An analysis relating stresses - which need not be elastic - orientation of the crystal axes, and relative retardation has been prepared. It is presented in the section immediately following the description of experimental techniques.

The succeeding section is concerned with the experimental verification of these analytical relationships. Briefly, the experiments have consisted in subjecting a single-crystal specimen, the orientation of whose crystal axes had been determined by back-reflection X-ray photographs, to a known state of stress. The relative retardation and extinction angle have then been measured. From these measurements the so-called stress-optical coefficients which appear in the theory can be determined. If the theory is correct, these quantities should be constant for a wide variety of crystal orientations and throughout the elastic and plastic stress ranges. This has been observed to be the case, at least within the limits of experimental error.

The fifth section of this report is concerned with experimental studies of polycrystalline specimens. In the first of these, specimens consisting of two differently oriented grains were subjected to tension at right angles to the grain boundary. These tests indicate that silver chloride is capable of providing clues to the manner of transmission of load across grain boundaries on a microscopic scale. A second series of tests has been concerned with observations on the progress of slip in a polycrystalline "transparent metal." These reveal also the existence of stress concentrations near the corners of grain boundaries, the importance of residual stresses, and further confirm the stress-optical theory first checked by the single-crystal tests.

The suitability of the photoelastic technique for the determination of stress concentration factors has been exploited in a series of tests reported in the sixth section. Single-crystal and polycrystal specimens with holes and notches have been subjected to progressively increasing tension. Although the number of tests reported is too small to permit definitive conclusions to be drawn, it appears that stress concentration factors for anisotropic materials may differ markedly from those for isotropic materials of the same shape. The initiation of yielding in polycrystalline specimens was made apparent by the appearance of surface lines which were continuous from grain to grain and which followed the same general pattern as that observed in the single-crystal tests.

This work was conducted at the University of Illinois under the sponsorship and with the financial assistance of the National Advisory Committee for Aeronautics.

SYMBOLS

Symbols are defined where they first appear in the text. This grouping is for the convenience of the reader.

a_o	reciprocal of the refractive index, $1/\eta$, nondimensional
$B_{11}, B_{12}, \ldots$	coefficients defining distorted indicatrix, nondimensional (see eq. (2))
$b_{11}, b_{12}, \ldots$	coefficients defining distorted indicatrix with reference to the x-, y-, and x-axes, nondimensional
$C_{11}, C_{12}, \ldots$	stress-optical coefficients defined by equation (3), sq in./lb
h	thickness of specimen, in.
l,m,n,	direction cosines, nondimensional
P	tension load applied to specimen in direction of Oy-axis, psi
X,Y,Z	Cartesian coordinates directed along principal crystal axes of a cubic crystal
x,y,z	arbitrary set of Cartesian axes; in general Ox has been taken along light ray and Oy has been taken as tension axis of specimen

α,θ	angles defining orientations of crystal axes (see eq. (21))
β	angle between Oy-axis and normal to boundary of specimen
Δ	relative retardations of polarized waves leaving specimen, in. or $m\mu$
Δ_1,Δ_2	absolute retardations of polarized waves in passing through specimen, in. or $m\mu$ (see eqs. (12))
ϵ_y	axial strain
η	average index of refraction for crystal, nondimensional
η_1,η_2	refractive indices of two polarized waves in crystal, nondimensional
λ	wave length of (monochromatic) light employed, in. or $m\mu$
ρ	radial coordinate in yz-plane
$\sigma_x,\sigma_y,\sigma_z,\tau_{xy},\tau_{xz},\tau_{yz}$	normal and shearing components of stress following usual notation, psi
σ_1	tangential principal stress at a point on a boundary, psi
φ	angular coordinate measured in yz-plane from y-axis; angles between Oy-axis and planes of polarization of transmitted light

EXPERIMENTAL TECHNIQUE

A variety of arrangements of optical equipment may be used for a polariscope suitable for observing silver-chloride specimens. It is desirable to have a polariscope capable of relatively high magnifications and a compensator which can accurately measure small retardations. Silver chloride is available commercially (Harshaw Chemical Co.) in the form of large single-crystal ingots or in the form of rolled polycrystalline sheets (1-, 1/2-, and 1/4-millimeter thicknesses are normal stock items). These sheets are very suitable for studies of polycrystalline specimens because they are easily recrystallized to give reasonably large grains which extend completely through the thickness

of the plate and have grain boundaries which are nearly normal to the plate surfaces. The surfaces of these rolled sheets are such that no polishing or other surface preparation is required even after heat treatment. There is no "edge effect" such as is exhibited by plastics. Creep is negligible at room temperature and experiments may be conducted over a period of 10 hours or longer.

Possibly the most convenient instrument for the present purpose is a large polarizing microscope. A wide variety of compensators and other convenient accessories are available for such instruments. In addition, these microscopes have a range of magnifications and a relatively large field of view. The present experimental work has been carried out using a Leitz SY polarizing microscope and a Berek compensator. With this microscope the field of view is only slightly under 1 centimeter in diameter at the minimum magnification of about 16X. Retardations were measured using a Berek compensator because of its sensitivity for small and medium phase differences. Quartz-wedge compensators of the Babinet type can be used with only a slight loss of accuracy. For convenience in taking photographs and in alining a light source, the microscope was mounted on the optical bench of a metallograph. Sources of both white and monochromatic light were available; however the latter was generally used. The monochromatic light (5,461 A) was obtained from an H-4 type lamp together with a No. 77 Wratten filter.

In the tests to be described, the specimens were subjected to pure tension loads by means of the small loading frame shown in figure 1. The specimen to be tested is held by clamps which are loaded through pins to assure an axial force. A bar linkage between the two clamps prevents the specimen from being twisted. The specimen is strained by turning a nut which is threaded with the screw rod connected to one of the specimen clamps. The applied load is determined from the reading of a 0.0001-inch Ames dial which actually measures the center deflection of a spring-steel beam which supports the other specimen clamp. This compact frame is mounted on a disk which can be screwed to the stage of the microscope. Sufficient longitudinal and transverse motion is available to enable any point of the specimen to be centered in the field of view. Also visible in figure 1 is the micrometer drum of the Berek compensator; this compensator slides into a slit in the microscope tube above the objective.

The test specimens used in the present investigation were generally about 0.04 inch (1 millimeter) thick, 0.28 inch wide, and 1.0 inch long. Polycrystalline specimens were cut from thin rolled plates of silver chloride with a jeweler's saw. The edges of these specimens were then polished on metallurgical abrasive papers with kerosene used as a lubricant. The preparation of single-crystal specimens is described in a later section of this paper. The

polycrystalline specimens were recrystallized and annealed using a technique described by Haynes (ref. 14). Silver chloride has a high coefficient of thermal expansion and is soft at elevated temperatures; consequently, care must be taken in the recrystallization and annealing process. The specimens were placed on a layer of finely ground quartz powder on the top of a glass-topped table in the center of a small thick-walled copper box. In this box they were heated to 740° F for about 3 hours after which they were cooled very slowly in the furnace. Examination of the annealed specimens in polarized light revealed that, for all practical purposes, they were entirely free from initial stress.

Where necessary for quantitative determinations of the stress state, the orientations of the specimen crystal axes were determined by back-reflection Laue X-ray photographs. The photographs were interpreted by means of a Greninger chart together with a Wulff stereographic net and a standard projection for a cubic crystal (ref. 15). This method can be used to determine the orientation of a single crystal or of an individual grain at the surface of an aggregate. The photographs are relatively easy to interpret and, with very simple equipment, yield accuracies of the order of 1°.

The experimental apparatus described was specifically chosen with a view to obtaining the greatest possible accuracy. Conventional polariscopes available in industrial and university stress-analysis laboratories can be adapted for research with silver chloride. If this is to be done, an accurate compensator must be used and the magnifying power of the polariscope will, in general, have to be increased. Some of the difficulties of the adaptation would be offset by the possibility of using thicker and larger specimens.

THEORY OF STRESS-OPTICAL EFFECT

Stress-optical effect in cubic crystals.- "What may be called the elementary theory of double refraction due to stress or strain, on the lines developed by F. E. Neumann, has been extended to natural crystals by F. Pockels in a series of memoirs (ref. 16) published in 1889 and 1890" (ref. 17). In these papers Pockels works with the relations between double refraction and strain. A complete treatment of the problem is given by Pockels in his "Lehrbuch der Kristalloptik" (ref. 18). In "A Treatise on Photo-Elasticity" (ref. 17), Coker and Filon present the theory in terms of the relations between double refraction and stress. However, no essential difference comes into question in their investigations, since perfect elasticity is assumed throughout.

Now let OX, OY, and OZ denote the principal axes of a cubic crystal; if a_o is the reciprocal of the refractive index, then the equation of the index ellipsoid[1] in the unstressed crystal is

$$a_o^2(X^2 + Y^2 + Z^2) = 1 \tag{1}$$

That is, the indicatrix in an unstressed cubic crystal is a sphere. Let the components of the applied stress, which may or may not be an elastic stress, referred to the three crystal axes be σ_X, σ_Y, σ_Z, τ_{XY}, τ_{XZ}, and τ_{YZ}. The effect of these stresses is to distort the indicatrix into an ellipsoid of the form

$$B_{11}X^2 + B_{22}Y^2 + B_{33}Z^2 + 2B_{12}XY + 2B_{31}ZX + 2B_{23}YZ = 1 \tag{2}$$

It is now assumed that the differences between the coefficients of this ellipsoid and the original sphere are small quantities of the first order, linear in the stresses. One has, in matrix notation,

$$\begin{bmatrix} B_{11} - a_o^2 \\ B_{22} - a_o^2 \\ B_{33} - a_o^2 \\ B_{23} \\ B_{31} \\ B_{12} \end{bmatrix} = \begin{bmatrix} C_{11} & C_{12} & C_{13} & C_{14} & C_{15} & C_{16} \\ C_{21} & - & - & - & - & - \\ C_{31} & - & - & - & - & - \\ C_{41} & - & - & - & - & - \\ C_{51} & - & - & - & - & - \\ C_{61} & - & - & - & - & C_{66} \end{bmatrix} \begin{bmatrix} \sigma_X \\ \sigma_Y \\ \sigma_Z \\ \tau_{YZ} \\ \tau_{ZX} \\ \tau_{XY} \end{bmatrix} \tag{3}$$

There are, therefore, 36 stress-optical coefficients[2] C_{ij} in the most general kind of crystal. In the present case, for cubic crystals, the axes OX, OY, and OZ are all equivalent. By symmetry one therefore has relations of the types $C_{66} = C_{44}$, $C_{33} = C_{11}$, and $C_{12} = C_{13} = C_{31}$.

---

[1]The surface here designated as the "index ellipsoid" or "indicatrix" is referred to as the Fresnel ellipsoid by Coker and Filon (ref. 17). Fresnel, however, deduced the wave surfaces from a single-surfaced ellipsoid having semiaxes equal to the velocities.

[2]These stress-optical coefficients are the same as the piezo-optical constants of Pockels (ref. 18) except for a logical reversal of sign; that is, $C_{ij} = -\pi_{ij}$.

Only three independent stress-optical coefficients remain and the above equations take on the forms

$$\left.\begin{aligned} B_{11} &= a_o^2 + C_{12}(\sigma_X + \sigma_Y + \sigma_Z) + (C_{11} - C_{12})\sigma_X \\ B_{22} &= a_o^2 + C_{12}(\sigma_X + \sigma_Y + \sigma_Z) + (C_{11} - C_{12})\sigma_Y \\ B_{33} &= a_o^2 + C_{12}(\sigma_X + \sigma_Y + \sigma_Z) + (C_{11} - C_{12})\sigma_Z \\ B_{23} &= C_{44}\tau_{YZ} \\ B_{31} &= C_{44}\tau_{XZ} \\ B_{12} &= C_{44}\tau_{XY} \end{aligned}\right\} \quad (4)$$

In the case of an isotropic material these equations must remain the same in form for any rotation of the coordinate axes; from this it follows that, for an isotropic material, $C_{44} = C_{11} - C_{12}$. (See, for instance, Coker and Filon, ref. 17, p. 293.)

In general, the stress components relative to the crystal axes are not known; however, these values can be readily determined if the stress components are known relative to any axes Ox, Oy, and Oz. The transformation equations are

$$\left.\begin{aligned} \sigma_X &= \sigma_x l_1^2 + \sigma_y m_1^2 + \sigma_z n_1^2 + 2(\tau_{xy} l_1 m_1 + \tau_{xz} l_1 n_1 + \tau_{yz} m_1 n_1) \\ \sigma_Y &= \sigma_x l_2^2 + \sigma_y m_2^2 + \sigma_z n_2^2 + 2(\tau_{xy} l_2 m_2 + \tau_{xz} l_2 n_2 + \tau_{yz} m_2 n_2) \\ \sigma_Z &= \sigma_x l_3^2 + \sigma_y m_3^2 + \sigma_z n_3^2 + 2(\tau_{xy} l_3 m_3 + \tau_{xz} l_3 n_3 + \tau_{yz} m_3 n_3) \\ \tau_{YZ} &= \sigma_x l_2 l_3 + \sigma_y m_2 m_3 + \sigma_z n_2 n_3 + \tau_{xy}(l_2 m_3 + l_3 m_2) + \\ &\quad \tau_{xz}(l_2 n_3 + n_2 l_3) + \tau_{yz}(n_2 m_3 + m_2 n_3) \\ \tau_{XZ} &= \sigma_x l_1 l_3 + \sigma_y m_1 m_3 + \sigma_z n_1 n_3 + \tau_{xy}(l_1 m_3 + l_3 m_1) + \\ &\quad \tau_{xz}(l_1 n_3 + n_1 l_3) + \tau_{yz}(n_1 m_3 + m_1 n_3) \\ \tau_{XY} &= \sigma_x l_1 l_2 + \sigma_y m_1 m_2 + \sigma_z n_1 n_2 + \tau_{xy}(l_1 m_2 + l_2 m_1) + \\ &\quad \tau_{xz}(l_1 n_2 + n_1 l_2) + \tau_{yz}(n_1 m_2 + m_1 n_2) \end{aligned}\right\} \quad (5)$$

in which (l_1, m_1, n_1), (l_2, m_2, n_2), and (l_3, m_3, n_3) are the direction cosines of OX, OY, and OZ, respectively, relative to the Ox-, Oy-, Oz-axes.

With these six stress components determined for any point in a crystal, and assuming that the stress-optical coefficients C_{11}, C_{12}, and C_{44} are known, it is easy to obtain the equation of the index ellipsoid relative to the crystal axes: That is, substitute the B_{ij}'s determined by equations (4) into equation (2).

It is desirable to be able to calculate the refractive indices and axes of polarization for a wave traveling, say, parallel to Ox. To determine these factors, the magnitude and direction of the semimajor and semiminor axes of the trace of the index ellipsoid in the zy-plane must be calculated. First the equation of the ellipsoid relative to Ox, Oy, and Oz is obtained by means of the transformation

$$\begin{bmatrix} X \\ Y \\ Z \end{bmatrix} = \begin{bmatrix} l_1 & m_1 & n_1 \\ l_2 & m_2 & n_2 \\ l_3 & m_3 & n_3 \end{bmatrix} \begin{bmatrix} x \\ y \\ z \end{bmatrix} \tag{6}$$

Now setting x equal to zero, the equation of the elliptic section of the indicatrix in the zy-plane is obtained. The principal semiaxes of this ellipse give the refractive indices and polarizing directions at the point.

If the coefficients of the index ellipsoid, when referred to Ox, Oy, and Oz are denoted by b_{11}, b_{12}, . . . then the section normal to Ox is

$$b_{22}y^2 + b_{33}z^2 + 2b_{23}yz = 1 \tag{7}$$

Or, upon setting $y = \rho \cos \varphi$ and $z = \rho \sin \varphi$, then

$$\frac{1}{\rho^2} = b_{22} \cos^2\varphi + b_{33} \sin^2\varphi + 2b_{23} \sin \varphi \cos \varphi \tag{8}$$

To obtain the directions of the principal axes of this ellipse set $(\partial\rho/\partial\varphi) = 0$; therefore,

$$\tan 2\varphi = \frac{2b_{23}}{b_{22} - b_{33}} \tag{9}$$

The values of φ obtained from equation (9) are the angles between the planes of polarization and the Oy-axis.

The magnitudes of the semiaxes of the trace of the indicatrix in the xy-plane are obtained by substituting the value of φ, given by equation (9), into equation (8). Consequently, there is obtained,

$$\rho_{\substack{\max \\ \min}} = \sqrt{2}\left[\left(b_{22} + b_{33}\right) \mp \sqrt{\left(b_{22} - b_{33}\right)^2 + 4b_{23}^2}\right]^{-1/2}$$

The refractive indices η_1 and η_2 of the two polarized waves passing through the crystal are equal to ρ_{max} and ρ_{min}, respectively. The square of the difference of the refractive indices is therefore

$$\left(\eta_1 - \eta_2\right)^2 = \frac{\left(b_{22} + b_{33}\right) - \sqrt{\left(b_{22} + b_{33}\right)^2 - \left[\left(b_{22} - b_{33}\right)^2 + 4b_{23}^2\right]}}{b_{22}b_{33} - b_{23}^2} \tag{10}$$

In an unstressed cubic crystal the equation of the section of the index ellipsoid normal to Ox is $a_o^2(y^2 + z^2) = 1$, where $1/a_o = \eta$ is the average index of refraction. When the crystal is stressed, this circle is deformed slightly to become the ellipse $b_{22}y^2 + b_{33}z^2 + 2b_{23}yz = 1$. Since the major and minor axes of this ellipse are nearly equal to the radius of the original circle, the coefficient b_{23} and the difference of the coefficients b_{22} and b_{33} must be very small quantities. In view of this, equation (10) can be simplified by using the first two terms of the binomial expansion of the square root. Also, the denominator of this equation is very closely a_o^4 or $1/\eta^4$. Equation (10), therefore, simplifies to

$$\eta_1 - \eta_2 = \frac{\eta^3}{2}\sqrt{\left(b_{22} - b_{33}\right)^2 + 4b_{23}^2} \tag{11}$$

It should be noted that the approximations just made follow directly from the assumptions upon which equations (3) are based.

If light is passed through a crystalline plate of thickness h, then the two resulting plane-polarized waves will have undergone

absolute retardations Δ_1 and Δ_2 given by

$$\left.\begin{aligned}\Delta_1 &= h(\eta_1 - 1)\\ \Delta_2 &= h(\eta_2 - 1)\end{aligned}\right\} \tag{12}$$

The relative retardation of the two polarized waves is, therefore,

$$\Delta = \Delta_1 - \Delta_2 = h(\eta_1 - \eta_2)$$

or, utilizing equation (12)(ref. 19),

$$\Delta = \frac{1}{2}\eta^3 h\sqrt{(b_{22} - b_{33})^2 + 4b_{23}^2} \tag{13}$$

The relative phase difference, measured in radians, is $2\pi\Delta/\lambda$, λ being the wave length "in vacuo."

Plane stress in a cubic crystal plate.- The experimental techniques of photoelasticity are best suited to the study of two-dimensional (plane-stress) problems. It is therefore desirable to proceed, on the basis of the foregoing theory, with a more detailed study of the generalized plane-stress problem.

Considering a single-crystal plate lying in the zy-plane, then, in the case of plane stress,

$$\sigma_x = \tau_{xy} = \tau_{xz} = 0 \tag{14}$$

Substituting these values into equations (5) and the resulting expressions for the stress components referred to the crystal axes into equations (4), the coefficients for the equation of the index ellipsoid are obtained in the forms

$$\left.\begin{aligned}
B_{11} &= a_o^2 + C_{12}(\sigma_y + \sigma_z) + (C_{11} - C_{12})(\sigma_y m_1^2 + \sigma_z n_1^2 + 2\tau_{yz} m_1 n_1)\\
B_{22} &= a_o^2 + C_{12}(\sigma_y + \sigma_z) + (C_{11} - C_{12})(\sigma_y m_2^2 + \sigma_z n_2^2 + 2\tau_{yz} m_2 n_2)\\
B_{33} &= a_o^2 + C_{12}(\sigma_y + \sigma_z) + (C_{11} - C_{12})(\sigma_y m_3^2 + \sigma_z n_3^2 + 2\tau_{yz} m_3 n_3)\\
B_{23} &= C_{44}\left[\sigma_y m_2 m_3 + \sigma_z n_2 n_3 + \tau_{yz}(m_2 n_3 + m_3 n_2)\right]\\
B_{31} &= C_{44}\left[\sigma_y m_1 m_3 + \sigma_z n_1 n_3 + \tau_{yz}(m_1 n_3 + m_3 n_1)\right]\\
B_{12} &= C_{44}\left[\sigma_y m_1 m_2 + \sigma_z n_1 n_2 + \tau_{yz}(m_1 n_2 + n_1 m_2)\right]
\end{aligned}\right\} \tag{15}$$

The equation of the index ellipsoid at a point in the stressed crystal is

$$B_{11}X^2 + B_{22}Y^2 + B_{33}Z^2 + 2B_{31}ZX + 2B_{23}YZ + 2B_{12}XY = 1 \tag{16}$$

The equation for the trace of this ellipsoid in the yz-plane is required; consequently, set $x = 0$ and substitute

$$\left.\begin{aligned} X &= m_1 y + n_1 z \\ Y &= m_2 y + n_2 z \\ Z &= m_3 y + n_3 z \end{aligned}\right\} \tag{17}$$

Equation (16) then becomes

$$\begin{aligned} &\left(B_{11}m_1^2 + B_{22}m_2^2 + B_{33}m_3^2 + 2B_{31}m_1m_3 + 2B_{23}m_2m_3 + 2B_{12}m_1m_2\right)y^2 + \\ &\left(B_{11}n_1^2 + B_{22}n_2^2 + B_{33}n_3^2 + 2B_{31}n_1n_3 + 2B_{23}n_2n_3 + 2B_{12}n_1n_2\right)z^2 + \\ &2\left[B_{11}m_1n_1 + B_{22}m_2n_2 + B_{33}m_3n_3 + B_{31}\left(m_1n_3 + m_3n_1\right) + \right. \\ &\left. B_{23}\left(m_2n_3 + m_3n_2\right) + B_{12}\left(m_1n_2 + m_2n_1\right)\right]yz = 1 \end{aligned} \tag{18}$$

This is an equation of the form of equation (7), that is, of the form $b_{22}y^2 + b_{33}z^2 + 2b_{23}yz = 1$. Using equations (15) for the B_{ij}'s and well-known relationships between the direction cosines involved, there are obtained

$$\left.\begin{aligned} b_{22} &= a_o^2 + C_{12}\left(\sigma_y + \sigma_z\right) + \left(C_{11} - C_{12} - C_{44}\right)\left[\sigma_y\left(m_1^4 + m_2^4 + m_3^4\right) + \right. \\ &\qquad \left.\sigma_z\left(m_1^2n_1^2 + m_2^2n_2^2 + m_3^2n_3^2\right) + 2\tau_{yz}\left(m_1^3n_1 + m_2^3n_2 + m_3^3n_3\right)\right] + C_{44}\sigma_y \\ b_{33} &= a_o^2 + C_{12}\left(\sigma_y + \sigma_z\right) + \left(C_{11} - C_{12} - C_{44}\right)\left[\sigma_y\left(m_1^2n_1^2 + m_2^2n_2^2 + m_3^2n_3^2\right) + \right. \\ &\qquad \left.\sigma_z\left(n_1^4 + n_2^4 + n_3^4\right) + 2\tau_{yz}\left(m_1n_1^3 + m_2n_2^3 + m_3n_3^3\right)\right] + C_{44}\sigma_z \\ b_{23} &= C_{44}\tau_{yz} + \left(C_{11} - C_{12} - C_{44}\right)\left[\sigma_y\left(m_1^3n_1 + m_2^3n_2 + m_3^3n_3\right) + \right. \\ &\qquad \left.\sigma_z\left(m_1n_1^3 + m_2n_2^3 + m_3n_3^3\right) + 2\tau_{yz}\left(m_1^2n_1^2 + m_2^2n_2^2 + m_3^2n_3^2\right)\right] \end{aligned}\right\} \tag{19}$$

These coefficients together with equations (9) and (13) give the polarization (extinction) angle φ and the relative retardation Δ, respectively.

In the case of a pure tension stress directed along the y-axis, the coefficients have the relatively simple form

$$\left.\begin{aligned} b_{22} - b_{33} &= \sigma_y\left[C_{44} + \left(C_{11} - C_{12} - C_{44}\right)\left(m_1^4 + m_2^4 + m_3^4 - m_1^2n_1^2 - m_2^2n_2^2 - m_3^2n_3^2\right)\right] \\ b_{23} &= \sigma_y\left(C_{11} - C_{12} - C_{44}\right)\left(m_1^3n_1 + m_2^3n_2 + m_3^3n_3\right) \end{aligned}\right\} \quad (20)$$

STUDY OF SINGLE CRYSTALS

Purpose of studying single crystals.- By applying a known state of stress to a plane crystal of known orientation, and by measuring the relative retardation of normally incident light waves, the foregoing theory can be checked experimentally. Such tests are necessary in order to establish the validity of the theory and to determine the numerical values of the stress-optical coefficients which appear in the stress-retardation equations. In practice, the simplest state of stress to analyze and to apply to a test specimen is pure tension. In the tests to be described, single-crystal specimens were subjected to pure tension loads, the orientations of the crystal axes were determined from back-reflection X-ray photographs, and the relative retardation and extinction angle were measured for a monochromatic light ray passing through the specimen. Measurements were made in both the elastic and plastic stress ranges. From these measurements the stress-optical coefficients can be determined. If the theory is correct, these coefficients should be constant throughout the elastic and plastic stress ranges and for any crystal orientation.

The verification obtained by these tension tests is not limited by the apparent simplicity of the stress state. Depending on its orientation, the crystal lattice is subjected to shear as well as to stretching when the specimen as a whole is in pure tension.

Preparation of test specimens.- Disks of clear silver chloride 3.25 inches in diameter and 0.3 inch thick were purchased from the Harshaw Chemical Co., Cleveland, Ohio. These disks contained large single crystals which were detected by lightly etching the surface with a sodium-thiosulfate solution. Single-crystal slices about 0.1 inch thick were cut from the disks with a jeweler's saw. The

specimens were then hand-polished on metallurgical abrasive papers (to 0000 fineness) utilizing kerosene as a lubricant. After washing the polished specimen in carbon tetrachloride, the surfaces were etched away by waving the specimen in a solution of sodium thiosulfate. The crystal specimens were then rinsed in water and blotted dry with clean filter paper. The resulting specimens were about 0.04 inch thick, 0.28 inch wide, and 1.0 inch long.

The crystals were annealed using the technique previously described in the section "Experimental Technique"; that is, they were heated to 740° F for about 3 hours, after which they were slowly cooled in the furnace. This heat treatment generally did not cause recrystallization but did, for all practical purposes, completely relieve the specimen of any internal stresses. The orientations of the crystal axes of each specimen were determined from back-reflection X-ray photographs as previously described. In some cases these photographs were taken both before and after the crystal was annealed. The heat treatment described did not affect the original orientations.

The cross-sectional dimensions of each annealed specimen were obtained using a micrometer caliper. Various reference lines were scratched lightly on one face of the specimen after which it was clamped in the small tension loading frame, as shown in figure 1. A small viselike clamp was used to hold the specimen grips in alinement and to prevent bending of the specimen as the clamping screws were tightened. In some cases stresses were introduced while clamping the specimen in this loading device; however, these were usually small.

Quantitative experimental results.- With the loading frame mounted on the stage of the microscope, a tensile load was applied to the specimen and various measurements were made. The angles from the direction of the applied load to the planes of extinction and subtraction ($\varphi + 45°$) were observed at various marked points. Using a Berek compensator, the relative retardations of monochromatic (5,461 A) light waves were measured at these same points. In addition to these measurements, strains in both the axial and transverse directions were measured using a screw-micrometer eyepiece. Measurements were made for loadings corresponding to stress increments of about 200 to 400 psi. The specimens were unloaded before each increase in load.

Stresses were computed based on the actual area of the strained specimen. This was determined by dividing the initial measured area by unity plus the measured axial strain. The observed retardations Δ were reduced to retardation per unit thickness Δ/h based on the actual thickness at the time of the observation. This thickness was determined by dividing the corrected area by the specimen width corrected in proportion to the measured transverse strain.

Eight groups of specimens were tested, each group having different orientations of the crystal axes relative to the principal stress and observation directions. For all except group I, the specimens had one crystal axis (OY) lying in the plane containing the axis of the specimen and the normal to the surface of the specimen, that is, in the xy-plane. The orientations of these specimens can therefore be described by two angles denoted α, the angle between the Oz- and the OZ-axis or between the xy-plane and the OX-axis, and θ, the angle between the Oy- and the OY-axis (both of which lie in the xy-plane). In matrix notation, the direction cosines defining the crystal orientation are then

$$\begin{bmatrix} l_1 & m_1 & n_1 \\ l_2 & m_2 & n_2 \\ l_3 & m_3 & n_3 \end{bmatrix} = \begin{bmatrix} \cos\alpha\cos\theta & \cos\alpha\sin\theta & -\sin\alpha \\ -\sin\theta & \cos\theta & 0 \\ \sin\alpha\cos\theta & \sin\alpha\sin\theta & \cos\alpha \end{bmatrix} \tag{21}$$

In general, retardations were measured at three points on the central cross section of the specimen. The average of these measurements (which were nearly equal) was then used to obtain a graph of stress against retardation such as that shown in figure 2. The linearity of the stress-retardation curve shown in this figure is typical of those obtained for all specimens in groups I, III, VII, and VIII, and also for specimens S-12 and S-13. The corresponding graphs for specimens of groups II and VI were more erratic; however, in these specimens the retardation was difficult to measure accurately because it was quite small and was superposed on a double set of prominent birefringent bands. The stress-retardation curves for specimens S-14 and S-22 showed a slight concavity upward, while those for specimens S-8 and S-9 were concave downward. Figure 3 (for specimen S-9) shows the most nonlinear relation obtained for stress against Δ/h. It should be regarded as exceptional, in the same way as figure 2 is typical.

In several cases relative retardations were measured during reloading of a plastically strained specimen. In each case the retardation per unit thickness agreed quite well with that measured during the initial loading.

The results of all of the tests are summarized in table I. The angles α and θ define the crystal orientation of each group as determined from the X-ray photographs. The average retardations per unit thickness were obtained directly from graphs such as are shown in figures 2 and 3.

Qualitative experimental results.- Before any load was applied to the annealed specimens, they appeared quite dark when examined between crossed Nicols. When a tensile load was applied, such that the stresses

were in the elastic range, considerable light was transmitted with almost uniform intensity over the whole specimen. The intensity of the light transmitted by the specimen depends on the magnitude of the applied load and, of course, on the orientation of the Nicols relative to the directions of the principal stresses.

The onset of plastic action was indicated in a dramatic way by the growth either of birefringent bands or of surface hairlines or both. The birefringent bands are caused by internal stresses remaining in the material after deformation by pencil glide. Generally, the birefringent bands are accompanied by surface lines; these are formed by the intersections of glide surfaces with the crystal surface. If the glide direction happens to be parallel to the surface, the lines are practically invisible. On the other hand, surface lines appear without birefringent bands if the glide surfaces overlap sufficiently.

Figure 4 shows the onset of plastic action in a typical specimen, S-10. In this case there were two glide systems operating simultaneously. The angles between the bands and the stress axis were 38° and -56°, measured in the plane of the specimen. There were no apparent surface glide lines at this load (440 psi), indicating that the glide directions were very nearly parallel to the surface of the crystal. In the present case the angle between the two glide directions was approximately 94°. This is substantially in agreement with Nye's conclusion (ref. 20) that the glide direction in silver chloride is $[\bar{1}10]$, since, in cubic crystals, the $[\bar{1}10]$ directions make angles of either 60° or 90° with each other. As the load was increased, other glide surfaces grew between those already present (see fig. 5). At still higher stresses the glide surfaces generally became so closely spaced and overlapping that the specimen appeared almost homogeneous.

In general, the specimens tested exhibited more than one set of glide surfaces as indicated by either birefringent bands or surface hairlines or both. Figure 6 shows a double system of surface lines observed in specimen S-22. This illustrates the development of surface lines without birefringent bands. A very interesting double system of glide surfaces was observed in single-crystal specimen S-12. In this case the two active sets of glide surfaces were distinctly separated as shown by figure 7(a). The relative retardations measured along the center cross section in the zones showing birefringent banding were considerably lower than those in the other zone, thus suggesting an unusual stress distribution over the cross section. Under still higher loading the two zones became very sharply separated as shown in figure 7(b). The differences in the directions of glide in the two zones are indicated by the distortions of the initially straight scratch lines on the surface of the specimen.

Comparison of experimental and theoretical results.- Before the theory discussed can be used to predict the optical effects in a stressed specimen, the stress-optical coefficients $\left(C_{11} - C_{12}\right)$ and C_{44} must be determined. In the present study these constants were determined such that the theoretical retardations would agree as closely as possible with the experimentally observed values. The correctness of the theory is vindicated by the fact that these two constants could be chosen such that the optical effects predicted by theory substantially agree with those observed for all of the specimens tested.

In table II the theoretical retardation coefficients and polarization angles are summarized for crystals oriented and stressed in the same way as the various groups of specimens tested. The values of the stress-optical coefficients used to compute the data given in this table were

$$C_{11} - C_{12} = -6.5(10)^{-8} \text{ sq in./lb}$$

and

$$C_{44} = 8.3(10)^{-8} \text{ sq in./lb}$$

The refractive index η was taken as 2.07, as given in the "International Critical Tables." The parameters Δ/h and φ were calculated using equations (13) and (9), respectively, together with equations (20). The dependence of these parameters on the crystal orientation is illustrated by figures 8 and 9. Also shown in these figures are the experimental results. Within the limits of experimental error, these agree with the theoretical predictions.

It is of some interest to speculate on the fundamental causes underlying the stress dependence of the photoelastic effect in a crystalline metallike material. That the photoelastic effect should in this case depend on stress rather than strain is not unreasonable. Mueller (ref. 21) has indicated three sources of birefringence in stressed ionic cubic crystals: The anisotropy of the Lorentz-Lorenz force, the anisotropy of the Coulomb forces, and the deformation of the crystal lattice which occurs when load is applied to the specimen. According to Mueller, this distortion of the lattice changes the energy levels and transition probabilities of the optical electrons, in this way altering the refraction of the atoms. It therefore produces a preferred orientation for polarized light, with accompanying retardation and other optical effects. As long as the behavior of the specimen is elastic, these optical effects will be in proportion to the load; this in turn will be proportional to either (macroscopic) stress or strain. Plastic deformation takes place when whole packets of molecules

glide relative to one another. Since this does not imply any further stretching of the lattice but only a relative motion of one lattice unit with respect to its neighbor, it may be inferred that in the plastic range the photoelastic effect in a ductile crystalline (or polycrystalline) material ought to be proportional to the stress rather than to the strain. This is what has actually been observed.

EXPERIMENTAL STUDY OF POLYCRYSTALLINE SPECIMENS

Tension tests of bicrystals.- The specimens here described as bicrystals were obtained by chance during the preparation of the single-crystal specimens previously described. During the annealing process two of these single-crystal specimens recrystallized in such a way that each consisted of two grains having their grain boundaries approximately on the center cross section of the specimen at right angles to the direction of pull. The orientations of the crystal axes of each grain in these two specimens were determined from X-ray photographs. The width and thickness of each specimen were measured and reference lines were lightly scratched onto one surface of each. The specimens were then clamped in the loading frame ready for testing. These two double-crystal specimens are referred to as D-1 and D-2; the letters L and R are used to designate their left- and right-hand grains. The orientations of the grains comprising these two specimens are presented in table III.

Relative retardations were measured at six points in each grain of each specimen at various stages of loading. The locations of the points at which the measurements were made are shown in the sketches in figures 10(a) and 10(b). These figures also show the relative retardations at the various points, plotted against the nominal stress (load divided by original area) applied to the specimen. In some cases, in order to avoid a congested diagram, only the average relative retardations have been plotted for points such as a, d, and e which are on cross sections somewhat removed from the grain boundary.

From figure 10(a) it is apparent that the stress distribution in the grains of specimen D-1 was not appreciably affected by the presence of the grain boundary. If a single crystal with the same orientation as D-1-L were subjected to a pure tension stress σ_y, then, on the basis of the theory previously described, the relative retardation would be, $\Delta = 0.491\sigma_y$ mμ/psi. The relative retardations observed for points in grain D-1-L are virtually in agreement with this value if only the nominal stress exists in the grain. Similarly, in grain D-1-R, the relative retardations observed are essentially equal to those caused by the nominal stress; in this case the theoretical relative retardation is $\Delta = 0.403\sigma_y$ mμ/psi. The observed extinction

angles in D-1-L and D-1-R were also essentially equal to the theoretical values of 26° and -6°, respectively, for pure tension stresses in the specimen. It may be inferred that in this specimen stresses were transmitted across the grain boundary with little or no local stress concentration at the boundary.

Inspection of figure 10(b) reveals that the stress distribution in specimen D-2 is not so simple as that observed in specimen D-1. However, this does not appear to be a result of the presence of the grain boundary but is believed to be a consequence of the way in which yielding occurred in one of the grains. In single-crystal specimen S-12 yielding occurred by dislocations in two distinctly separated glide surfaces as has been described in a foregoing section. Yielding of grain L of specimen D-2 appeared to progress in very much the same way as had been observed in specimen S-12; that is, gliding took place on two sets of surfaces which did not overlap appreciably. In one of the zones so formed the retardations, and therefore the stresses, were higher than the average, while in the other they were lower.

The general appearance of grain D-2-L after plastic yielding is shown by figures 11(a) and 11(b). From figure 11(a) it can be seen that points a, e, and f lie in one type of zone while b and c lie in another and d is on the boundary between these zones. The relative retardations measured at points a, e, and f were the lowest observed in this grain while those at b and c were the highest. The non-uniformity of stress in grain D-2-R, indicated by the relative retardation measurements, is probably a direct consequence of the unusual stress distribution in grain D-2-L. If only a pure tension stress existed throughout specimen D-2, the relative retardations theoretically would be $\Delta = 0.217\sigma_y$ mμ/psi for grain L and $\Delta = 0.191\sigma_y$ mμ/psi for grain R. These values agree reasonably well with the average relative retardations measured on the various cross sections; however, in view of the unusual stress distribution, the average obtained from the limited number of measurements made probably does not accurately represent the average for the section.

Tension tests of specimens with many crystals.- Several polycrystalline specimens of silver chloride were tested in simple tension in order that a qualitative understanding of the stress distribution in the grains of such specimens might be obtained. The specimens were cut from thin rolled sheets of silver chloride, after which they were recrystallized and annealed by heat treatment as previously described. The test to be described was performed on a specimen 0.375 inch wide and 0.0197 inch thick. The specimen was subjected to a pure tension load which was increased in 1-pound increments; each increment corresponded to an average tension stress increment of 135 psi. After each increase in load the relative retardation was measured near the centers of each of three grains, the locations of which are indicated in figure 12(a).

Before any load was applied, the recrystallized specimen was free from all but very small internal stresses. When viewed between crossed Nicols, the specimen appeared quite dark except for some reflection from grain boundaries which were not quite normal to the faces of the specimen. Under a 1-pound load, fairly high stress concentrations were observed near the corners of some grains. However, the retardation over the interior portion of each grain was almost constant, indicating that distant from the boundaries the stress distribution is fairly homogeneous. As the load was increased to 2 pounds, some surface glide lines became visible near the loading clamps; however, no signs of plastic action were visible near the center of the specimen. With a 3-pound load, some glide lines appeared on the surfaces of several grains. From the photograph of figure 12(b), which was taken after the removal of this load, it is apparent that yielding resulted in residual stresses, especially along the grain boundaries.

As the load was increased, plastic action occurred in all grains, as is evidenced by the birefringent bands and surface lines in figure 12(c). Of especial interest are the surface lines in the largest grain (grain C); the lines in the lower portion of this grain are directed differently from those in the upper portion. In grain B the situation is similar; the surface lines in the upper portion of the grain are continuous with those in grain A, while in the lower portion they are not. It is also apparent that the relative retardation now varies considerably throughout any particular grain. The magnitude of this variation in grain A under a load P of 5 pounds is shown in figure 13. At this loading the surface of the specimen appeared, to the unaided eye, much like a sheet of cellophane which has been crinkled and then stretched. The grain boundaries appeared as sharply defined creases. The birefringence pattern obtained after removal of the 5-pound load indicates that quite large residual stresses were present. Some grains now showed a streaky birefringence pattern which was not always directed parallel to the surface lines.

For tension loads greater than about 6 pounds (810 psi) comparatively large strain was required in order to obtain a 1-pound load increase. At these higher loads the relative retardation at different points in any grain varied considerably; because of this, the mean values determined for grains A, B, and C may be somewhat in error. In figure 14 the relative retardations near the centers of these grains are plotted against the applied load. It is important to note that these relative retardations are approximately proportional to the load even when the strain is relatively large, in further verification of the stress-optical theory previously established by means of single-crystal tests. Those grains (notably B and C) which showed a discontinuity in their glide lines were observed to form an irregular surface near this discontinuity. This surface, which appears somewhat like a grain boundary, can be seen in figure 15 which shows the specimen

under a load of 10 pounds (1,350 psi). Under this load the specimen was necked slightly. The color of restored white light approached that of the first-order yellow.

EXPERIMENTAL STUDY OF NOTCHED SPECIMENS

Single-crystal specimens.- The technique previously described can be used to study the state of stress in the neighborhood of a circular hole in a single-crystal specimen subjected to a tension load. The stresses may be in either the elastic or plastic ranges; consequently, the redistribution of stress resulting from yielding may be studied.

A single-crystal specimen with a hole drilled through its center was polished and annealed in the manner previously described. The orientations of the crystal axes of this specimen were the same as those of grain R of specimen D-1 (see table III). The specimen was 0.278 inch wide and 0.0365 inch thick, and the hole was 0.068 inch in diameter. Relative retardations were measured, at various stages of loading, at each of the points indicated in the sketch given in figure 16. At some loadings additional measurements were made as close as possible to the boundary of the hole.

When subjected to the first load increment (1.6 pounds), the specimen showed no signs of plastic yielding; however, when this load was removed, there was evidence of some residual stress. Under a load of about 2 pounds, surface hairlines were observed near points b and c. As the load was increased, these lines increased in number and prominence. When the load reached 2.6 pounds, birefringent bands appeared at the 45° points around the hole; these bands were all approximately at an angle of 45° with the direction of the applied load.

The extinction patterns observed as the polarizer and analyzer were rotated simultaneously are shown in figures 17(a) to 17(d). From these figures it is evident that the stress distribution changes very rapidly near the boundary of the hole. It should be remembered that the extinction angle depends on the orientations of the crystal axes as well as on the directions and relative magnitudes of the principal stresses. Figures 17(a) to 17(d) would therefore be different for specimens with different crystal orientations. The surface lines, the birefringent banding, and the extinction pattern near the boundary of the hole are clearly shown in figure 17(e). The birefringent bands were more easily seen when the specimen was unloaded as is shown in figure 17(f). The orientations of the crystal axes of the present specimen (N-5) were the same as those of grain D-1-R given in table III. Using this information and the stress-optical constants for silver chloride, there is found, for specimen N-5,

$$\left.\begin{aligned} 2b_{23} &= \left(-1.53\sigma_y + 16.35\tau_{yz} + 0.98\sigma_z\right) \times 10^{-8} \\ b_{22} - b_{33} &= \left(-6.32\sigma_y - 2.51\tau_{yz} + 2.50\sigma_z\right) \times 10^{-8} \end{aligned}\right\} \quad (22)$$

Now let β be the angle from the y-axis (load axis) to the normal to the boundary of the specimen at some point on a boundary and let σ_1 be the nonzero principal stress at this point. Then

$$\left.\begin{aligned} \sigma_y &= \sigma_1 \sin^2\beta \\ \sigma_z &= \sigma_1 \cos^2\beta \\ \tau_{yz} &= -\sigma_1 \sin\beta \cos\beta \end{aligned}\right\} \quad (23)$$

The data in table IV have been obtained by substituting equations (22) and (23) into equations (9) and (13). Since the specimen was 0.0365 inch thick, it follows that the principal stress σ_1, in pounds per square inch, is 9.06 times the relative retardation Δ, in millimicrons, at boundary points for which $\beta = 0$; 2.86Δ at boundary points for which $\beta = 45^\circ$; and 3.73Δ at boundary points for which $\beta = 90^\circ$. In general, the principal stress at a point on the boundary of a specimen is proportional to the relative retardation at the point. The constant of proportionality depends on the orientations of the crystal axes relative to the boundary and the plane of the specimen.

In figure 16 the relative retardations at various points in the specimen are plotted as a function of the load. Although yielding was noted at a load of about 2 pounds, there appeared to be no redistribution of the stresses until the load exceeded 4 pounds. Increasing the load beyond 4 pounds seemed to have practically no effect on the stress level at points a and d; however, it caused the stresses at points b and c to increase slightly more rapidly than they had previously.

The extinction angles observed at points a, b, c, d, and h were essentially in agreement with those given in table IV for $\beta = 90^\circ$. The extinction angles observed at points e and f were -7° and 17°, respectively, whereas the theoretical values for $\beta = -45^\circ$ and 45° were -34° and 43°, respectively. These differences indicate that e and f are so far from the boundary of the hole that the principal stress direction is not parallel to the boundary and the second principal stress is not zero.

At loads of 3.65 and 4.7 pounds relative retardations were measured at several additional points on the center cross section. In particular,

measurements were made as close as possible to the edge of the hole. The distribution of stress determined from these measurements is shown in figure 18. It is interesting that the stress concentration factors, based on the nominal stress on the gross area of the specimen, are only of the order of 2.25. The corresponding concentration factor for a similar specimen but of isotropic, elastic material is theoretically 3.24 (ref. 22). In the present case, however, this factor is probably a function of the orientations of the crystal axes. Also, the measurements were made slightly in from the edge of the hole after some plastic yielding had occurred; consequently, the experimentally determined factor may be somewhat low. Basically, however, the large difference between stress concentration factors of 3.25 and 2.25 must be attributed to the fact that silver chloride is not isotropic. Since structural metals also have this property, the further investigation of this effect would appear to be very desirable.

The distribution of stress around the rim of the hole is illustrated in figure 19. In interpreting the diagram, tension stresses are to be measured radially outward from the edge of the hole and compression stresses, radially inward. Also shown in this figure is the corresponding curve obtained experimentally by Coker and Filon (ref. 17) for an isotropic, elastic material (cellulose nitrate). Again the stress concentration factor obtained for the isotropic material is considerably larger than that obtained for the particular crystal specimen under study.

Polycrystalline specimens.- Several polycrystalline specimens containing either a central hole or edge notches were tested in order that their behavior might be qualitatively observed. In each of these specimens the notches or holes were of such size that the gross area of the specimen was reduced by about 21 percent. As these specimens were loaded, birefringent bands or surface lines were noted when the nominal stress, based on the gross area, was about 200 psi. Generally, yielding was first evidenced by the appearance of surface lines extending from the hole or notch boundary into the specimen along the section of minimum area. The influence of grain orientation on the direction of these lines in the vicinity of the critical cross section seemed to be of a secondary nature. In most cases the surface lines in this area were continuous from grain to grain and followed the same general pattern as that observed in the single-crystal specimen, N-5 (see fig. 17(f)). Some of these surface lines can be seen in figures 20(a) to 20(c). Relative retardations were measured at the centers of a number of grains in these specimens. These measurements indicated that there was no large redistribution of stress as the yield point was passed.

CONCLUDING REMARKS

Tests of single-crystal specimens of silver chloride have shown that the optical effect in this crystalline metallike material is a measure of the stress state (and not of the state of strain). The experimental data obtained from these tests have checked the accuracy, in both the elastic and plastic ranges, of a general theory which quantitatively relates optical effects to the stress state. In addition, these tests have provided data necessary for the determination of the so-called stress-optical coefficients which appear in the theory. Silver chloride appears to be a suitable material for photoelastic studies of the effects of plastic yielding on the state of stress in a crystalline material.

To avoid any possibility of misunderstanding, it should be stated plainly that, while silver chloride does possess the significant property of being an aggregate of ductile crystals, it is not apt to be exactly identical in its glide mechanism with any particular structural metal. Grain-boundary phenomena may also be expected to differ as between silver chloride and, say, an aluminum alloy. For these reasons inferences based on silver-chloride tests will always require verification by means of experiments performed on the metals themselves. Such experiments if made blindly are apt to be costly and inefficient. It is felt that an optically active material can play a useful role as a guide to further experimentation. It can also serve as a check on theories of the plastic state.

Experiments reported herein on bicrystals and on specimens having stress-raisers are not sufficiently numerous to permit drawing dogmatic conclusions. It appears certain, however, that stress concentration factors in actual crystalline materials are not the same as those in the isotropic materials usually considered in the mathematical theory of elasticity. The feasibility of making significant experiments in complicated stress fields has been demonstrated. It must be considered, however, that all of these tests have been performed on thin specimens. In an actual structural element the grain would be supported by neighbors on its sides as well as its edges.

University of Illinois,
Urbana, Ill., February 7, 1953.

REFERENCES

1. Fried, B.: Some Observations on Photoelastic Materials Stressed Beyond the Elastic Limit. Proc. Soc. Exp. Stress Analysis, vol. VIII, no. 2, 1951, pp. 143-148.

2. Fried, Bernard: The Solution of Fluid Flow Problems Through Analysis of the Optical Birefringence Accompanying Such Flow. Contract NAw-5109, NACA and Wash. State College, 1948.

3. Hetényi, M.: A Study in Photoplasticity. Proc. First U. S. Nat. Cong. Appl. Mech. (June 1951, Chicago, Ill.), A.S.M.E., 1952, pp. 499-502.

4. Moeller, R. D., Schonfeld, F. W., Tipton, C. R., Jr., and Waber, J. T.: A Metallurgical Investigation of Silver Chloride. Trans. A.S.M., vol. 43, 1951, pp. 39-69.

5. Tammann, G.: Change in Qualities of Nonmetallic Substances on Cold Working. Naturwiss., vol. 20, 1932, pp. 958-960.

6. Stepanov, A. V.: The Plastic Properties of AgCl and NaCl Crystals. Phys. Zs. Sowjetunion, vol. 8, 1935, pp. 25-40.

7. Fugassi, P., and McKinney, D. S.: The Preparation of Silver Chloride Films. Rev. Sci. Instr., vol. 13, no. 8, Aug. 1942, pp. 335-337.

8. Fetters, K. L., and Dienes, M.: AgCl as a Medium for Study of Ingot Structures. Tech. Pub. No. 1570, Metals Tech., vol. 10, Aug. 1943.

9. Orowan, E.: Classification and Nomenclature of Internal Stresses. Symposium on Internal Stresses in Metals and Alloys, Monograph and Report Series, No. 5, Inst. Metals, 1947, pp. 47-60.

10. Nye, J. F.: Photoelastic Investigation of Internal Stresses in AgCl Caused by Plastic Deformation. Nature, vol. 161, no. 4088, Mar. 6, 1948, pp. 367-368.

11. West, C. D., and Makas, A. S.: Technical Crystals With Abnormally Large Stress Birefringence. Jour. Chem. Phys., vol. 16, no. 4, Apr. 1948, p. 427.

12. Stepanov, A. V.: New Optical Method for Study of Stresses by Polarized Light. Zhurnal Tekhnicheskoi Fiziki, vol. 19, 1949, pp. 205-217.

13. Prigorovskii, N. I.: Contemporary Development of an Optical Polarization Method for Determination of Stresses. Zavodskaya Laboratoriya, vol. 15, 1949, pp. 305-321.

14. Haynes, J. R.: Technique for Obtaining Increased Range and Mobility of Free Electrons in Silver Chloride. Rev. Sci. Instr., vol. 19, no. 1, Jan. 1948, p. 51.

15. Barrett, Charles S.: Structure of Metals. First ed., McGraw-Hill Book Co., Inc., 1943, p. 167.

16. Pockels, F.: Ueber den Einfluss elastischer Deformationen, speciell einseitigen Druckes, auf das optische Verhalten krystallinischer Körper. Ann. Phys. und Chemie, Neue (dritte) Folge, Bd. 37, Heft 5, 1889, pp. 144-172; Heft 6, 1889, pp. 269-305; Heft 7, 1889, pp. 372-395; Ueber die durch einseitigen Druck hervorgerufene Doppelbrechung reguläre Krystalle, speciell von Steinsalz und Sylvin. Ann. Phys. und Chemie, Neue (dritte) Folge, Bd. 39, Heft 3, 1890, pp. 440-469.

17. Coker, E. G., and Filon, L. N. G.: A Treatise on Photo-Elasticity. The Univ. Press (Cambridge), 1931, p. 288.

18. Pockels, F.: Lehrbuch der Kristalloptik. B. G. Teubner (Leipzig), 1906.

19. Nye, J. F.: Plastic Deformation of Silver Chloride, Part I. Proc. Roy. Soc. (London), ser. A, vol. 198, no. 1053, Aug. 15, 1949, pp. 190-204.

20. Nye, J. F.: Plastic Deformation of Silver Chloride, Part II. Proc. Roy. Soc. (London), ser. A, vol. 200, no. 1060, Dec. 22, 1949, pp. 47-66.

21. Mueller, H.: Theory of the Photoelastic Effect of Cubic Crystals. Phys. Rev., vol. 47, no. 12, ser. 2, June 15, 1935, pp. 947-957.

22. Howland, R. C. J.: On the Stresses in the Neighbourhood of a Circular Hole in a Strip Under Tension. Phil. Trans. Roy. Soc. (London), ser. A, vol. 229, no. 671, Jan. 6, 1930, pp. 49-86.

TABLE I.- SUMMARY OF EXPERIMENTAL RESULTS

Group	Orientation		Specimen	Av. $\Delta/h\sigma_y$, sq in./lb	Av. φ, deg
	α, deg	θ, deg			
[a]I	12.5	12	S-1	20.1×10^{-8}	73
			S-3	20.8	73
			S-10	21.1	72
II	57	30	S-4	9.8	24
III	57	50.5	S-5	31.3	12
			S-7	30.0	14
IV	57	39	S-8	20	11
			S-9	20	8
			S-12	18.5	12
V	22.5	0	S-13	29.8	85
			S-14	28.7	83
			S-22	29.0	86
VI	22.5	25.5	S-15	6.7	80 $\mp$
			S-16	5.7	Varied
VII	22.5	68	S-19	29.5	32
			S-21	29.5	33
VIII	22.5	89	S-17	31.8	43

NACA

[a]Angles α and θ given for group I are only approximate. Calculations are based on the following measured orientation:

$$\begin{bmatrix} l_1 & m_1 & n_1 \\ l_2 & m_2 & n_2 \\ l_3 & m_3 & n_3 \end{bmatrix} = \begin{bmatrix} 0.959 & 0.187 & -0.215 \\ -0.212 & 0.973 & -0.099 \\ 0.191 & 0.141 & 0.971 \end{bmatrix}$$

TABLE II.- SUMMARY OF ANALYTICAL RESULTS

Orientation as for group	Orientation		$\Delta/h\sigma_y$, sq in./lb	φ, deg
	α, deg	θ, deg		
I	12.5	12	23.4×10^{-8}	74.8
II	57	30	5.3	17.5
III	57	50.5	30.9	10.6
IV	57	39	18.8	9.5
V	22.5	0	28.9	90.0
VI	22.5	25.5	6.0	77.1
VII	22.5	68	29.4	31.6
VIII	22.5	89	33.0	41.5

NACA

TABLE III.- ORIENTATIONS OF GRAINS IN

SPECIMENS D-1 AND D-2

Specimen	Grain L	Grain R
	$\begin{bmatrix} l_1 & m_1 & n_1 \\ l_2 & m_2 & n_2 \\ l_3 & m_3 & n_3 \end{bmatrix}$	$\begin{bmatrix} l_1 & m_1 & n_1 \\ l_2 & m_2 & n_2 \\ l_3 & m_3 & n_3 \end{bmatrix}$
D-1	$\begin{bmatrix} 0.999 & -0.031 & 0 \\ 0.016 & 0.510 & 0.860 \\ 0.027 & 0.860 & -0.510 \end{bmatrix}$	$\begin{bmatrix} 0.919 & 0.040 & 0.393 \\ -0.026 & 0.998 & -0.052 \\ -0.395 & 0.040 & 0.918 \end{bmatrix}$
D-2	$\begin{bmatrix} 0.725 & -0.578 & 0.375 \\ 0.656 & 0.741 & -0.136 \\ -0.208 & 0.341 & 0.917 \end{bmatrix}$	$\begin{bmatrix} 0.626 & -0.609 & 0.487 \\ 0.443 & 0.792 & 0.420 \\ -0.643 & -0.004 & 0.766 \end{bmatrix}$

TABLE IV.- STRESS-OPTICAL RELATIONS AT A BOUNDARY OF SPECIMEN N-5

β, deg	$\Delta/h\sigma_1$	φ, deg
0	11.9×10^{-8}	10.7
45	37.6	42.8
-45	37.8	-34.0
90	28.9	6.8

NACA

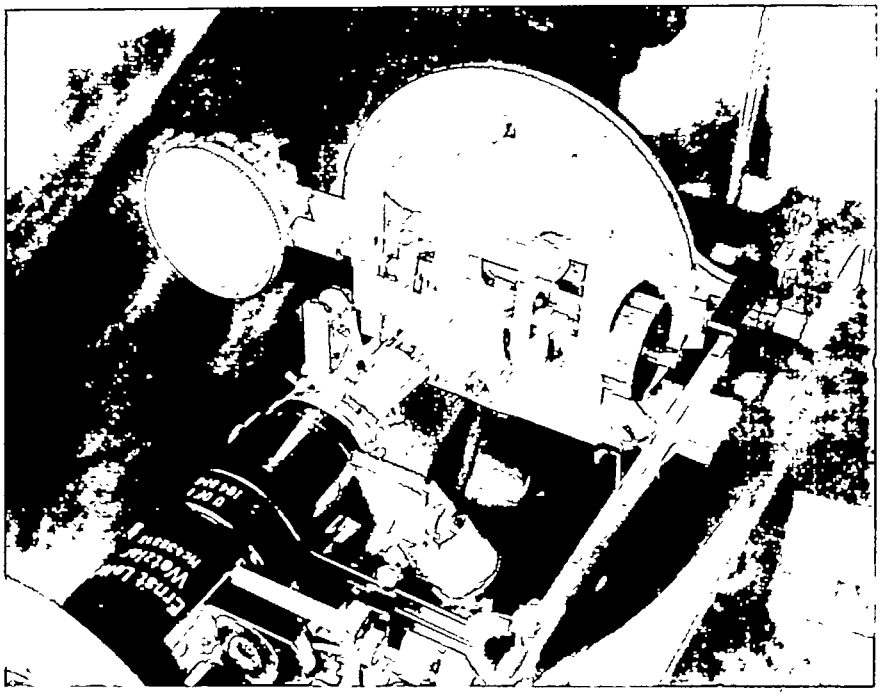

L-81197

Figure 1.- Apparatus (on microscope stage) for applying tension loads to specimens.

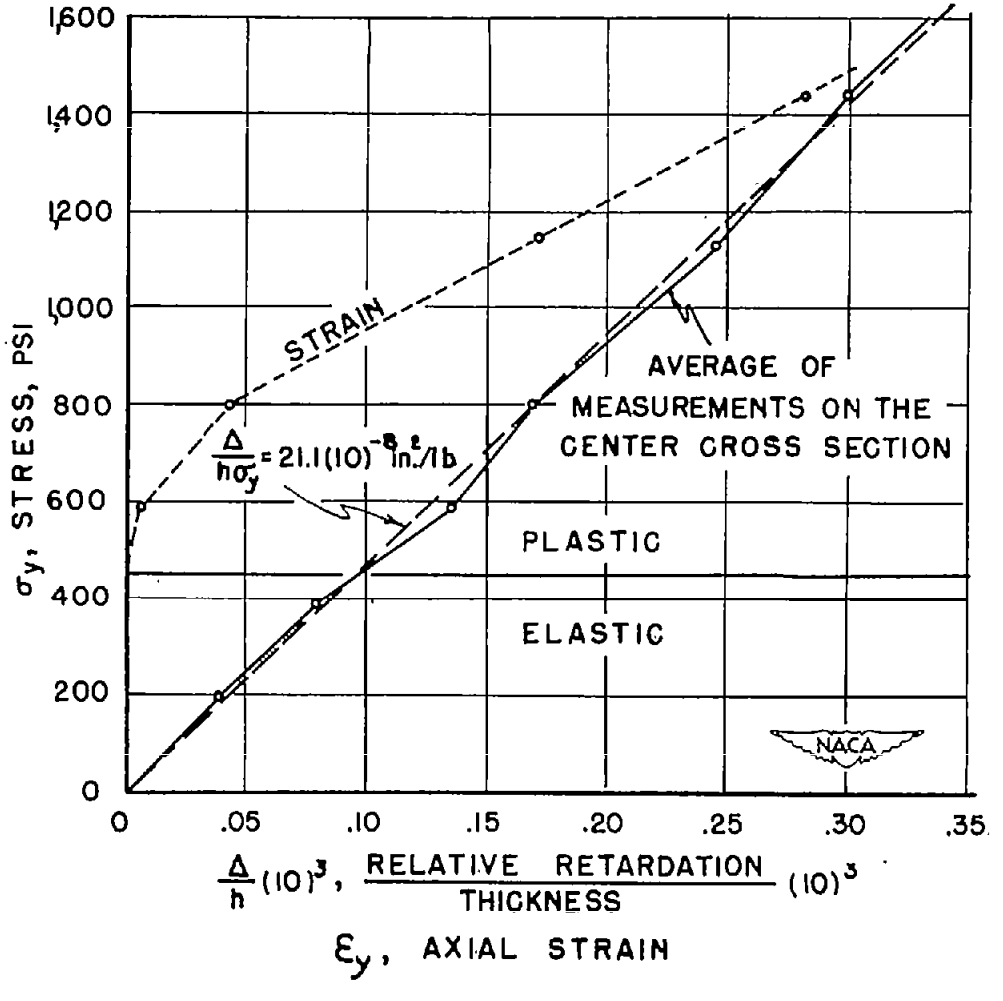

Figure 2.- Typical curve of relative retardation against stress. Specimen S-10.

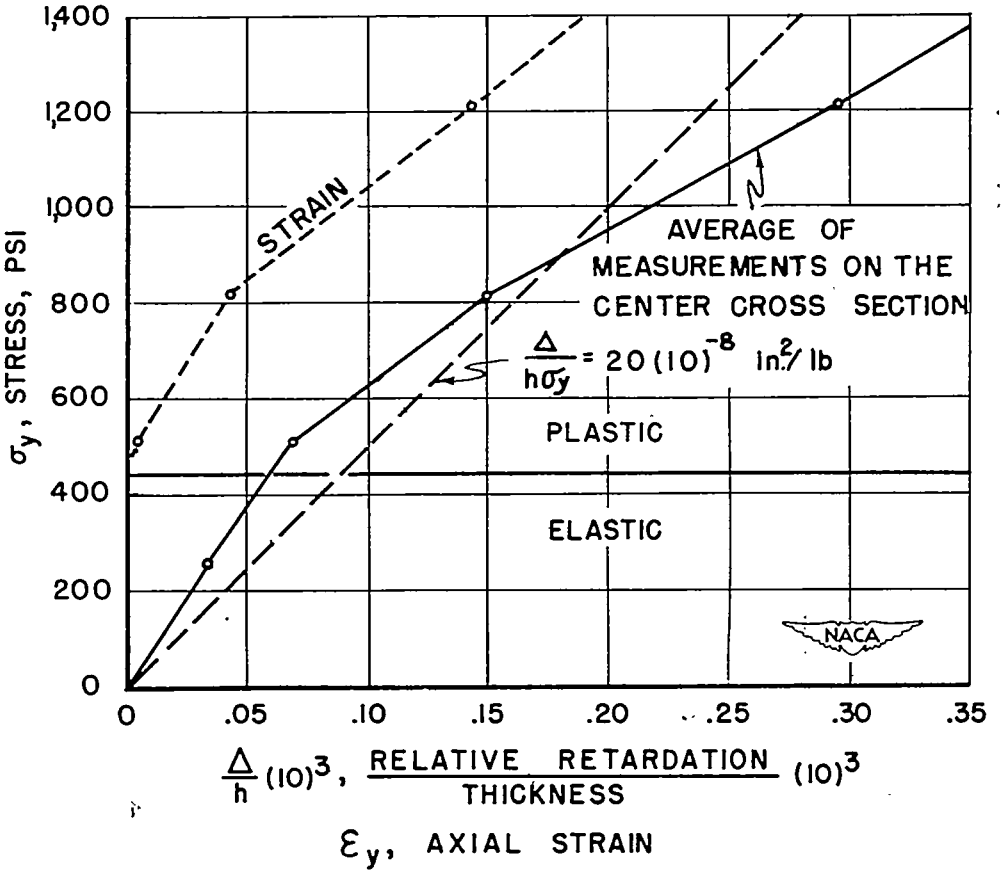

Figure 3.- Relative retardation against stress for specimen S-9. This specimen showed the least linear stress-optical effect.

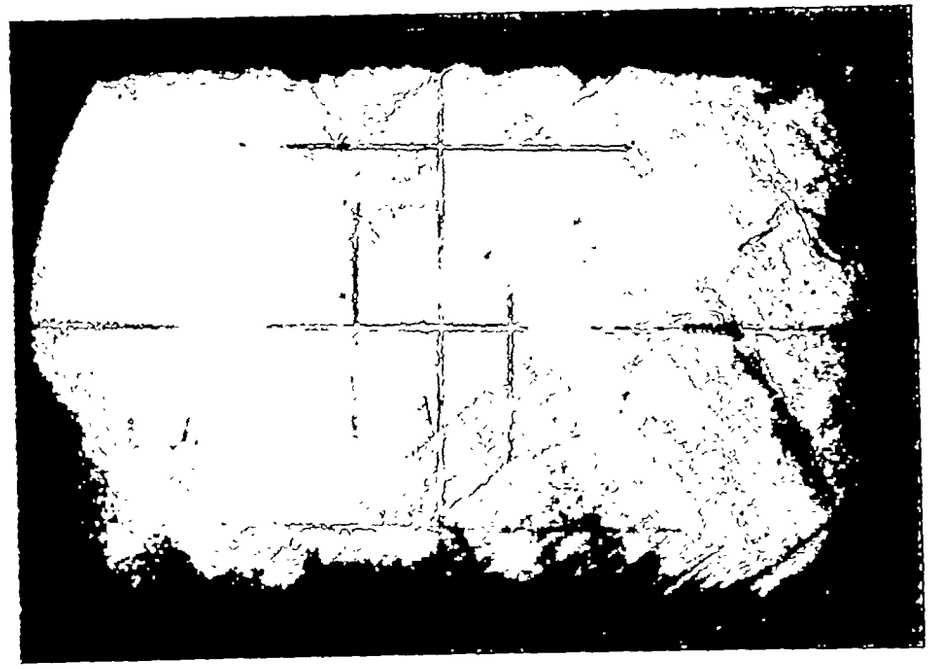

L-81198

Figure 4.- Start of yielding in specimen S-10. Stress, 440 psi; Nicols at -9° and 81° to (horizontal) load direction; X12.

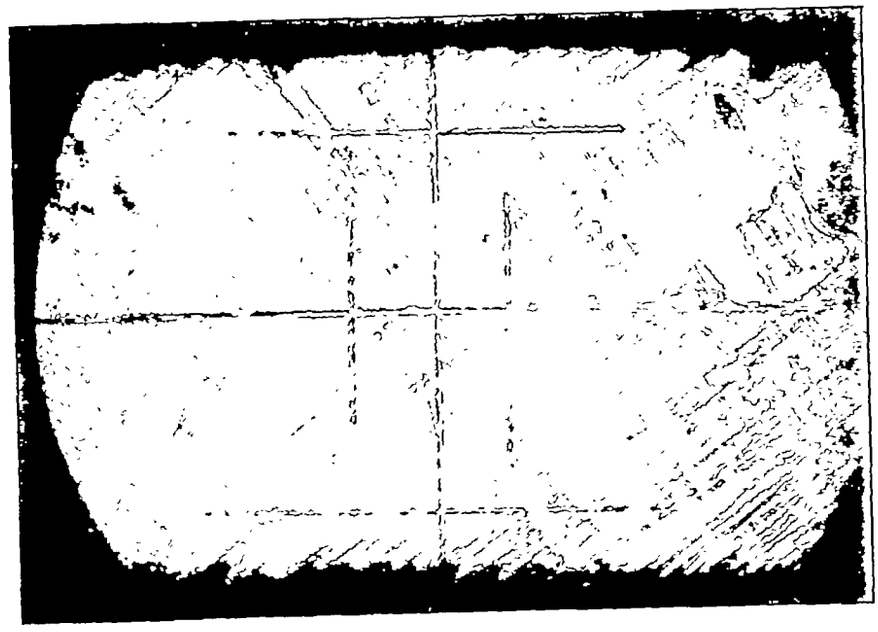

L-81200

Figure 5.- Glide bands in specimen S-10. Stress, 490 psi; Nicols at -9° and 81° to (horizontal) load direction; X12.

L-81199

Figure 6.- Surface lines in specimen S-22. Stress, 580 psi; Nicols horizontal and vertical; load applied horizontally; X36.

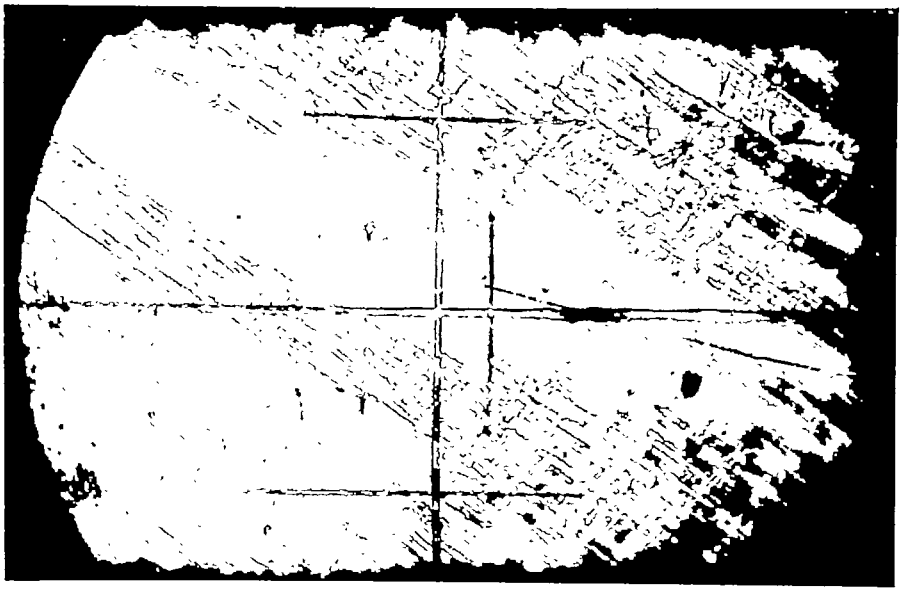

L-81201

(a) Stress, 590 psi.

Figure 7.- Double system of glide surfaces in specimen S-12. Nicols horizontal and vertical; load applied horizontally; X12.

L-81202

(b) Stress, 1,300 psi.

Figure 7.- Concluded.

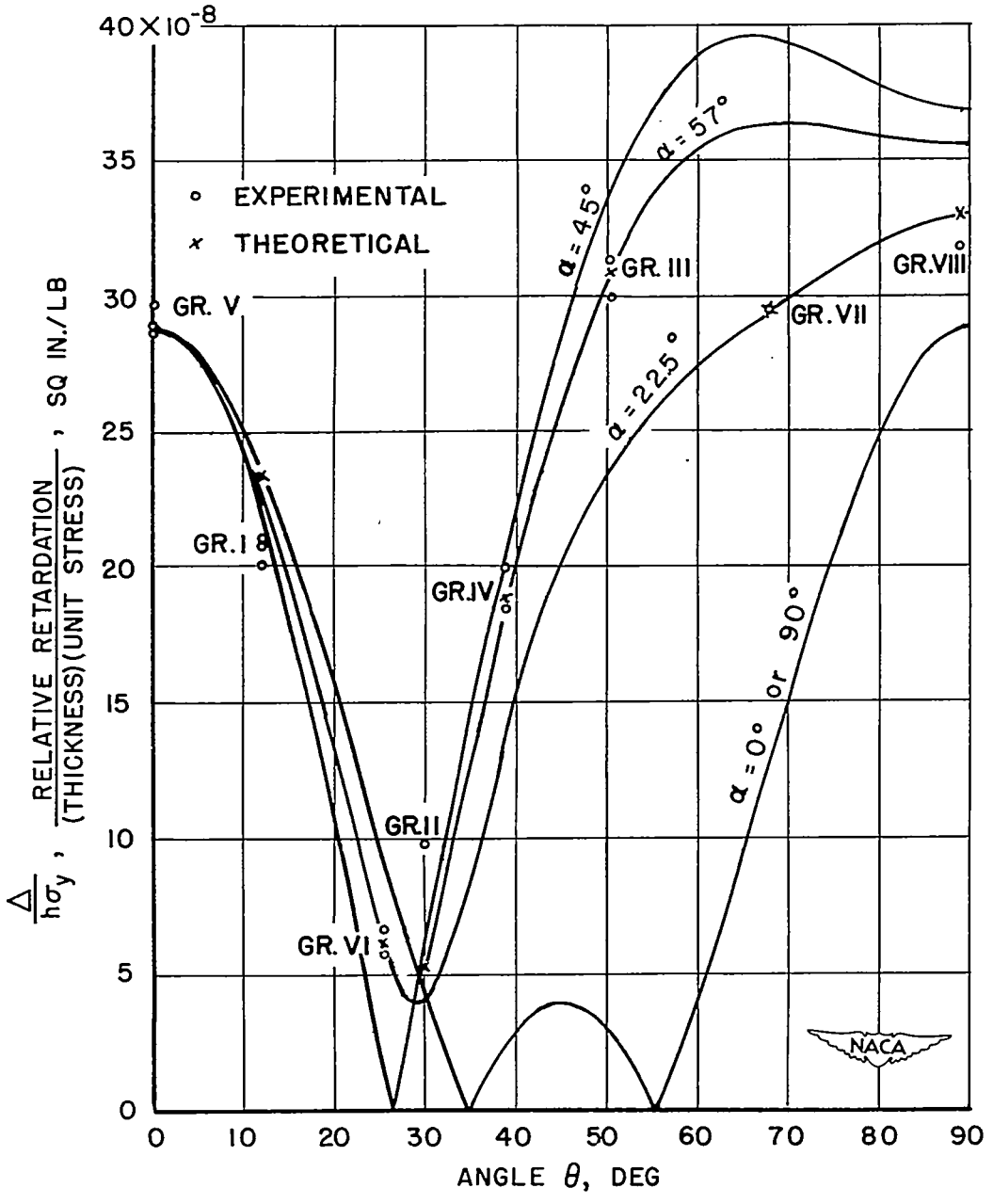

Figure 8.- Dependence of relative retardation on crystal orientation for uniaxial stress. $C_{11} - C_{12} = -6.5 \times 10^{-8}$ square inch per pound; $C_{44} = 8.3 \times 10^{-8}$ square inch per pound.

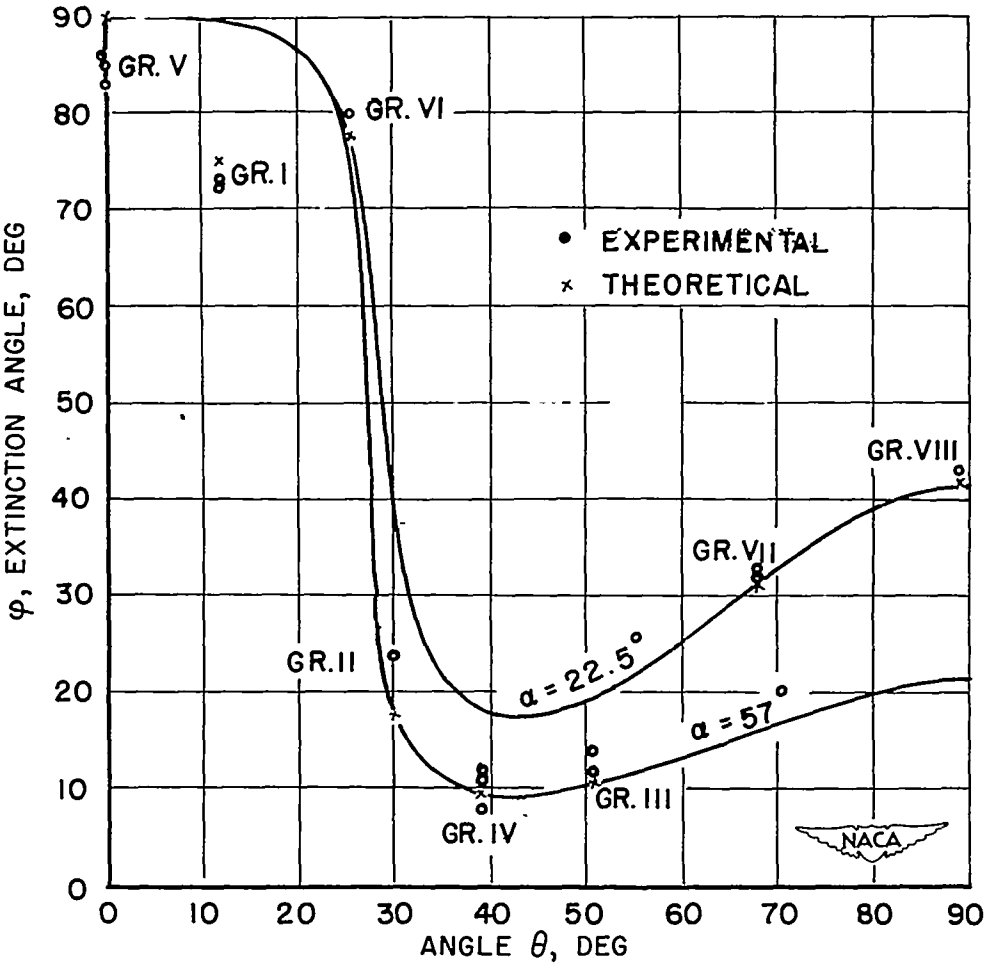

Figure 9.- Dependence of extinction angle on crystal orientation for uniaxial stress. $C_{11} - C_{12} = -6.5 \times 10^{-8}$ square inch per pound; $C_{44} = 8.3 \times 10^{-8}$ square inch per pound.

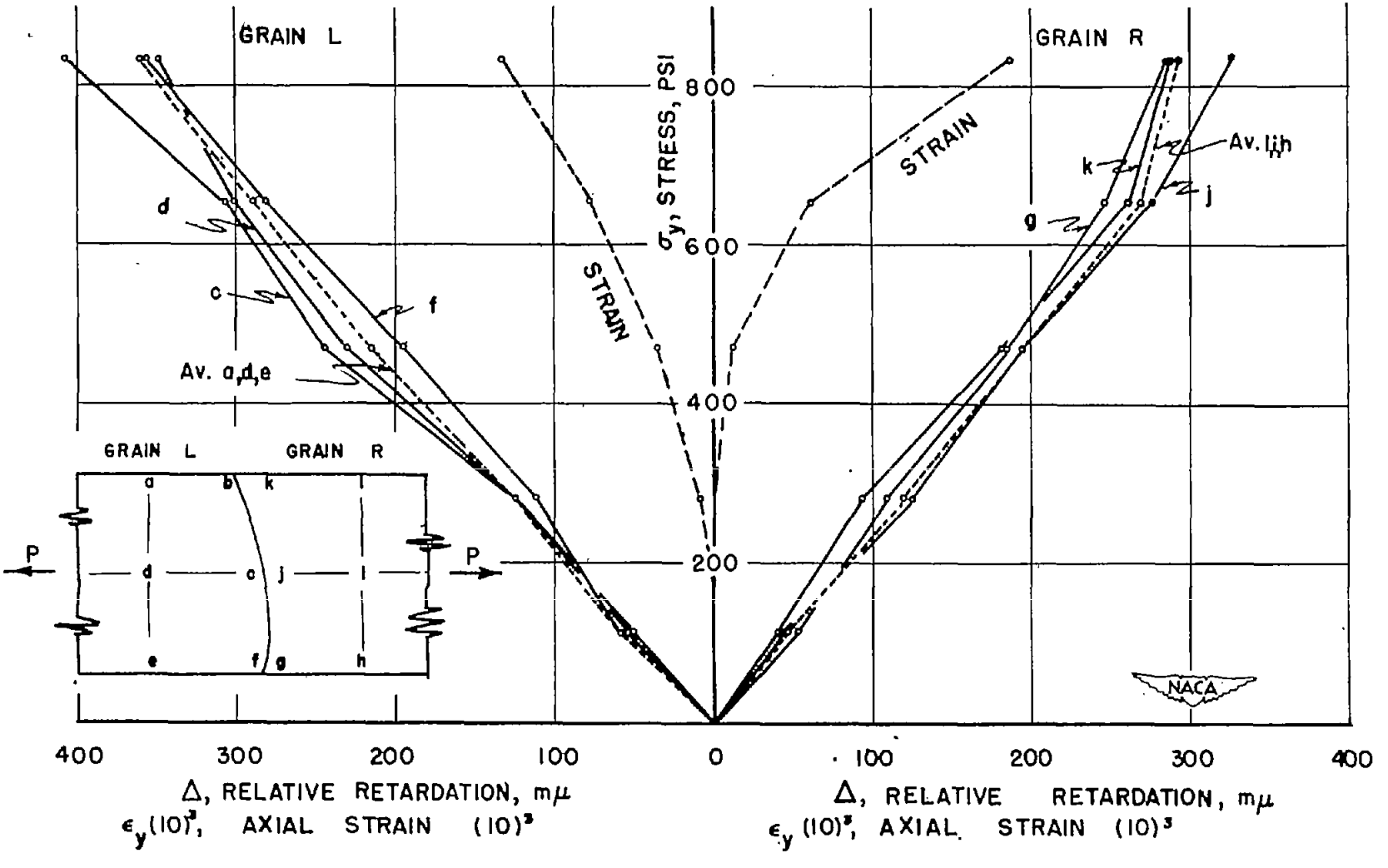

(a) Specimen D-1. Thickness, 0.055 inch; width, 0.264 inch; area, 0.0145 square inch.

Figure 10.- Relative retardation against nominal stress.

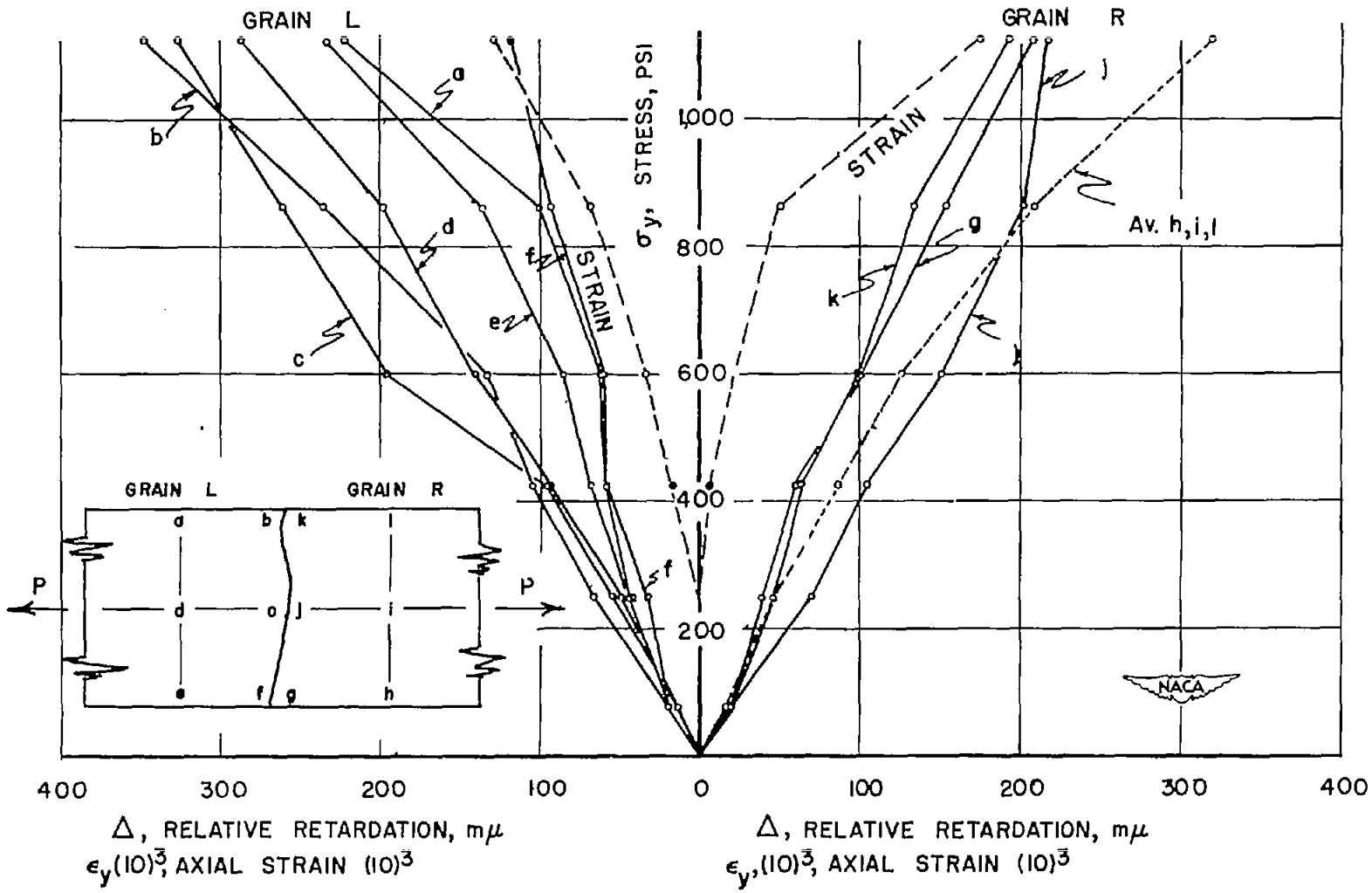

(b) Specimen D-2. Thickness, 0.038 inch; width, 0.0260 inch; area, 0.0099 square inch.

Figure 10.- Concluded.

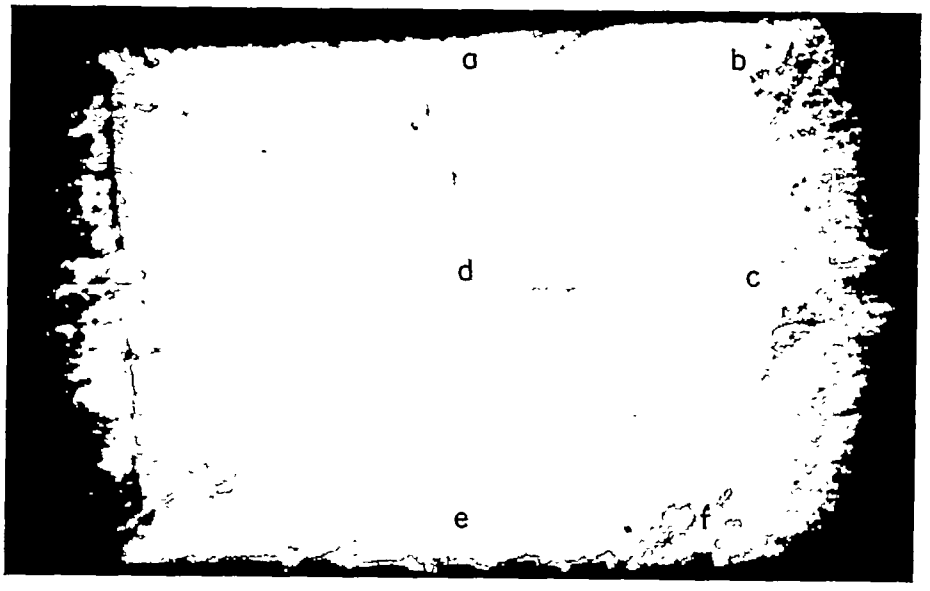

(a) Points a, b, c, d, e, and f. X12.3.

L-81203.1

(b) Point d. X39.3.

Figure 11.- Appearance of grain L of specimen D-2 after plastic yielding. Stress, 860 psi; Nicols horizontal and vertical; load applied horizontally.

(a) 1.0-pound load applied horizontally.

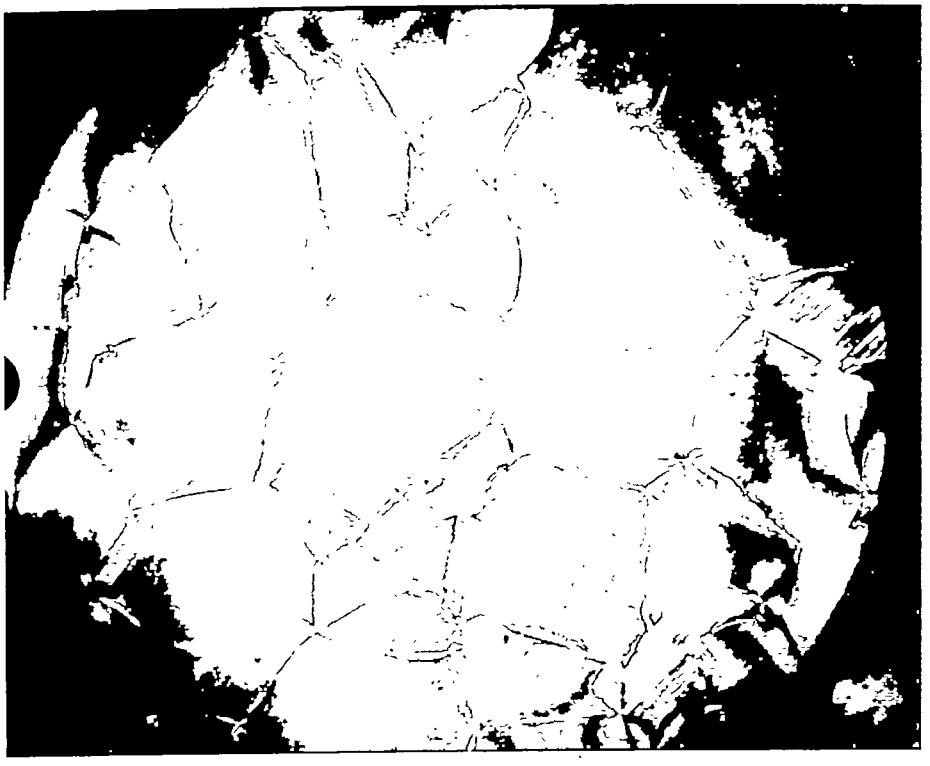

L-81204

(b) Unloaded from 3.0 pounds.

Figure 12.- Specimen P-10. Nicols horizontal and vertical; X12.3.

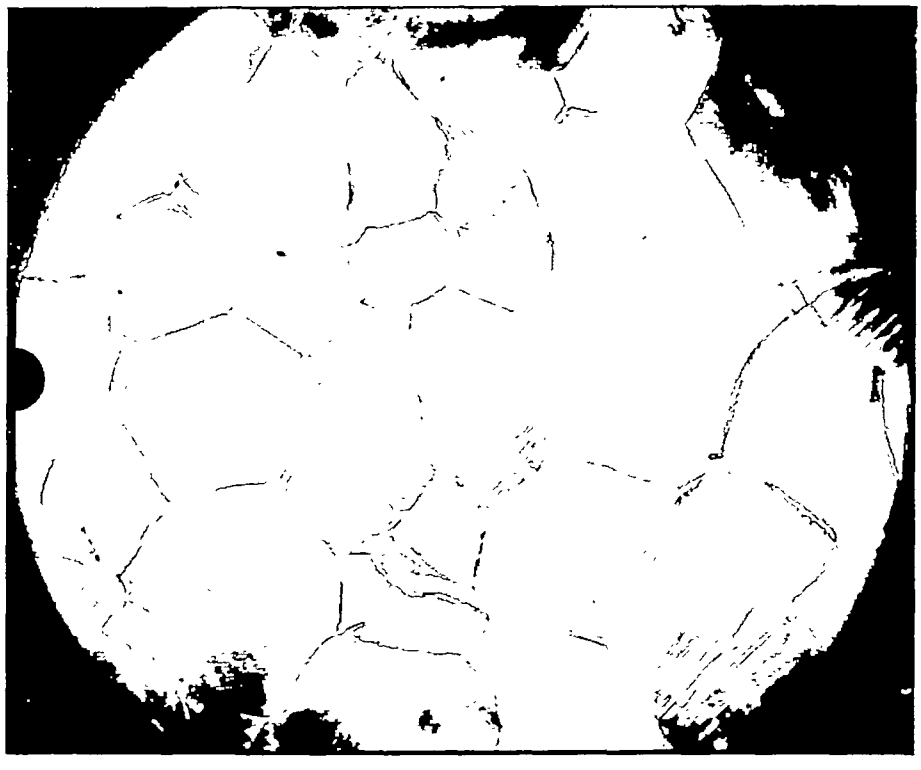

L-81205

(c) 5.0-pound load applied horizontally.

Figure 12.- Concluded.

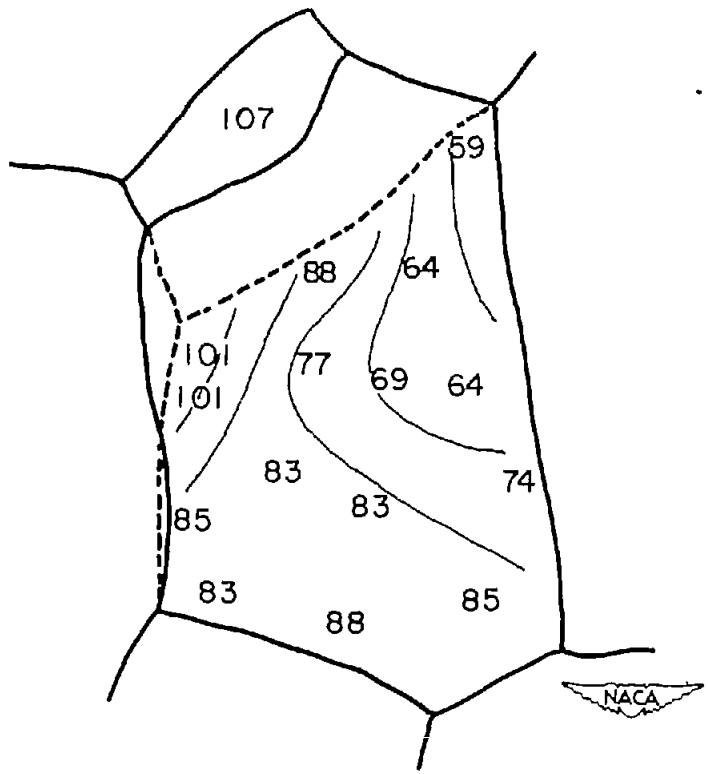

Figure 13.- Variation of relative retardation in grain A of specimen P-10. P = 5.0 pounds. Numbers indicate retardation at the point in millimicrons.

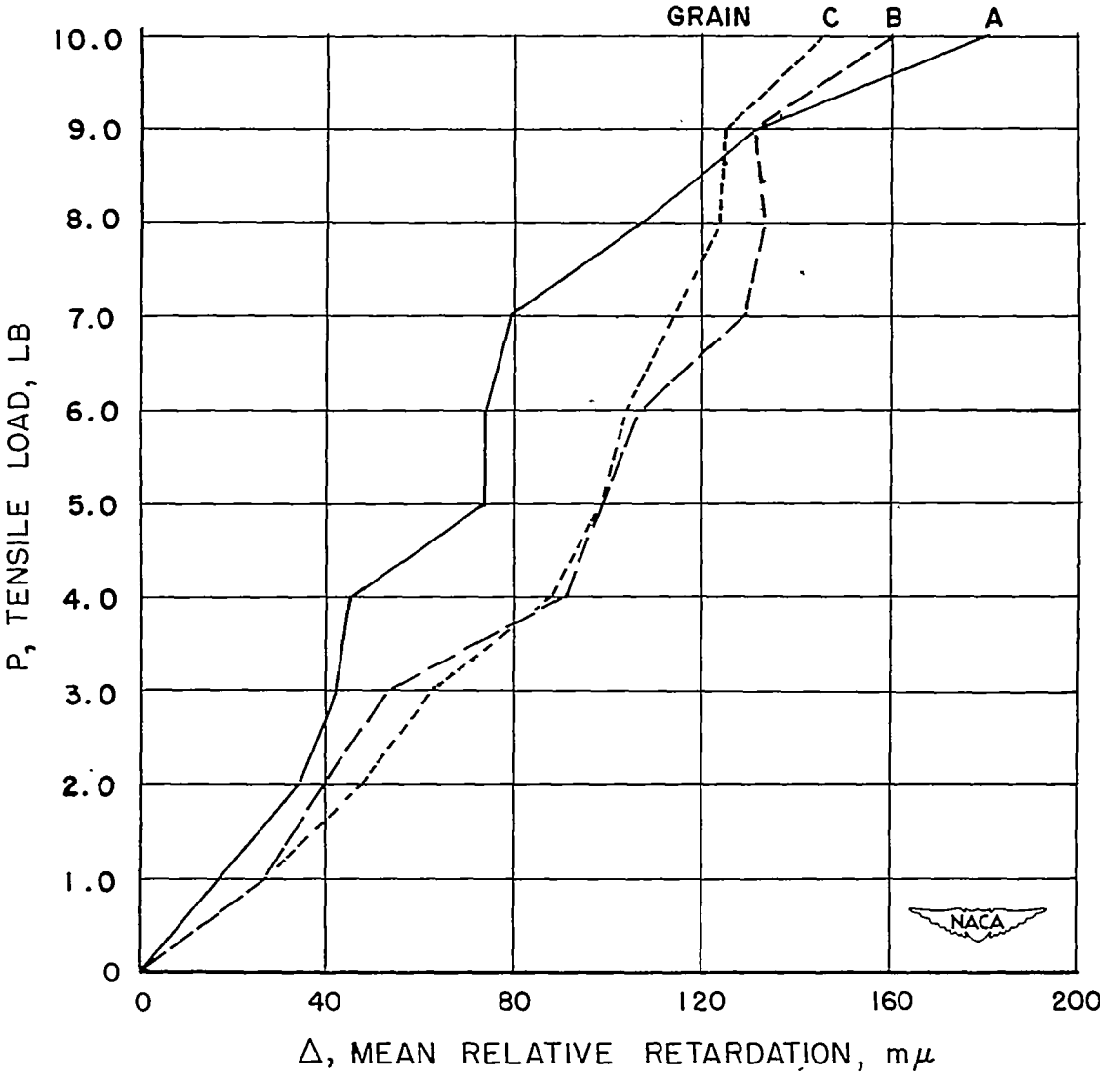

Figure 14.- Load against mean relative retardation for specimen P-10. Specimen 0.375 inch wide and 0.0197 inch thick.

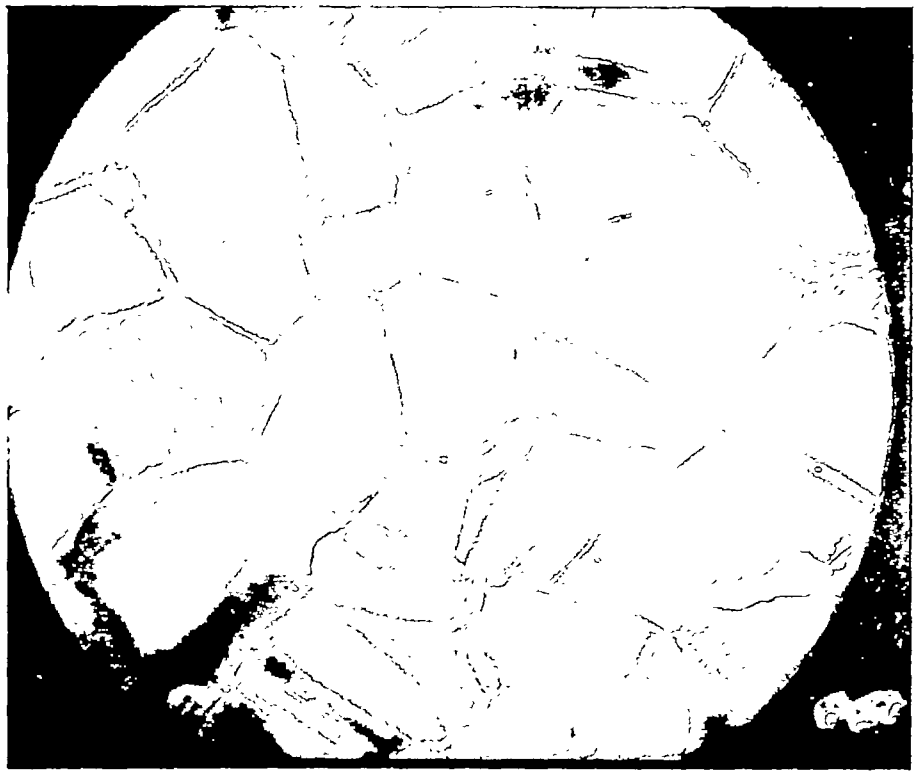

L-81206

Figure 15.- Specimen P-10. 10.0-pound load applied horizontally. Nicols horizontal and vertical; X12.3.

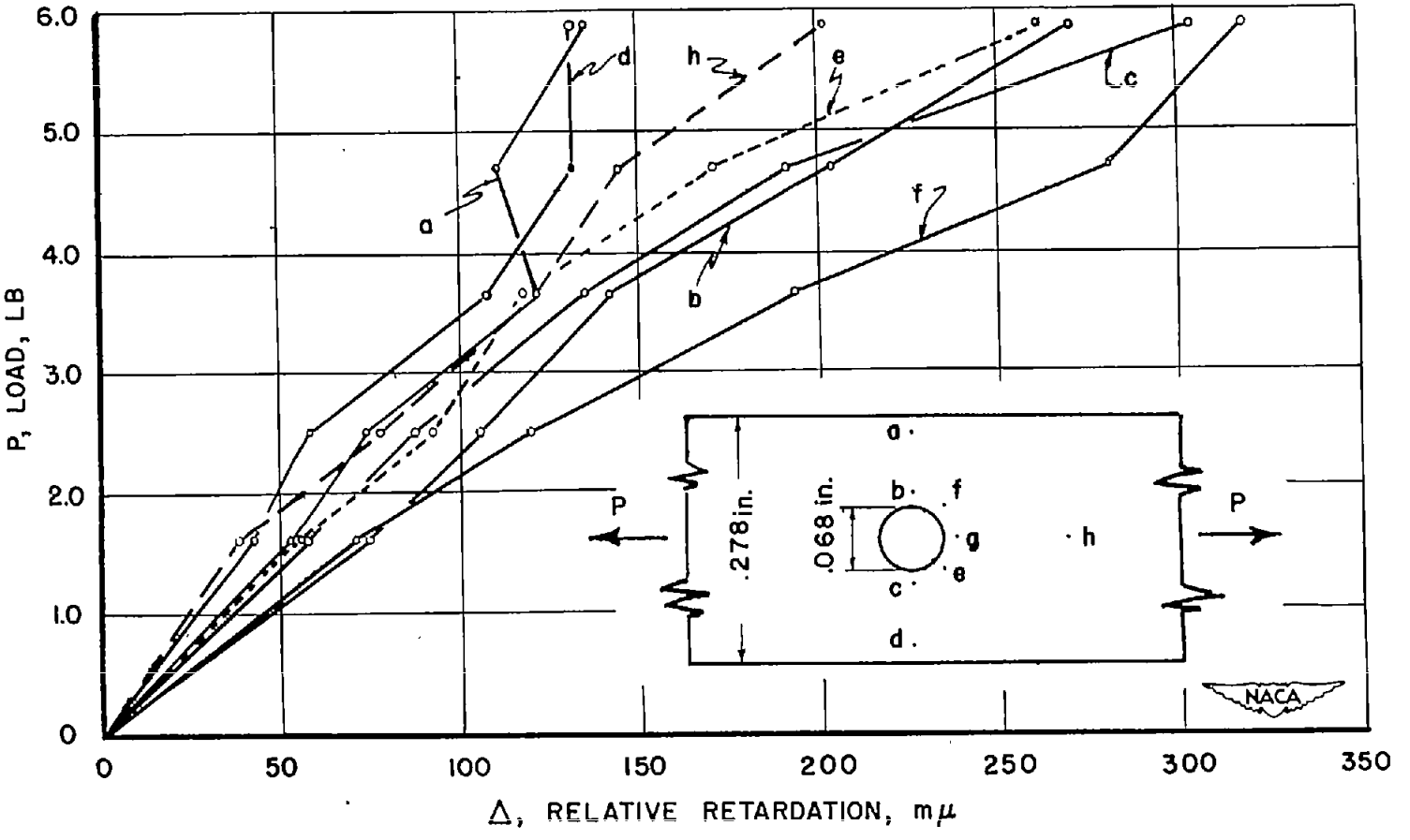

Figure 16.- Relative retardation against load for specimen N-5.

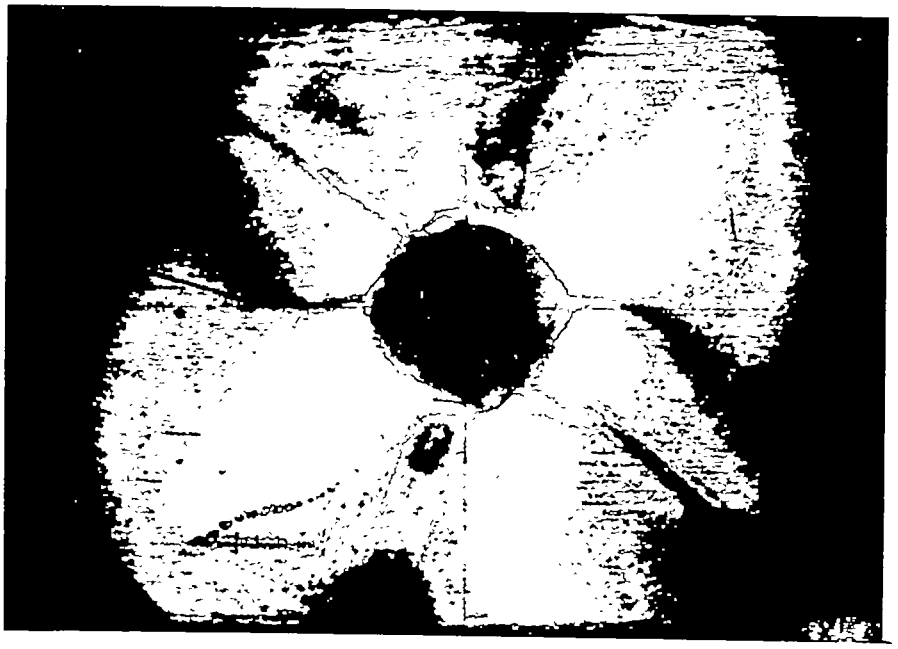

(a) 2.6-pound load applied horizontally; Nicols at 0° and 90° to the load; X12.

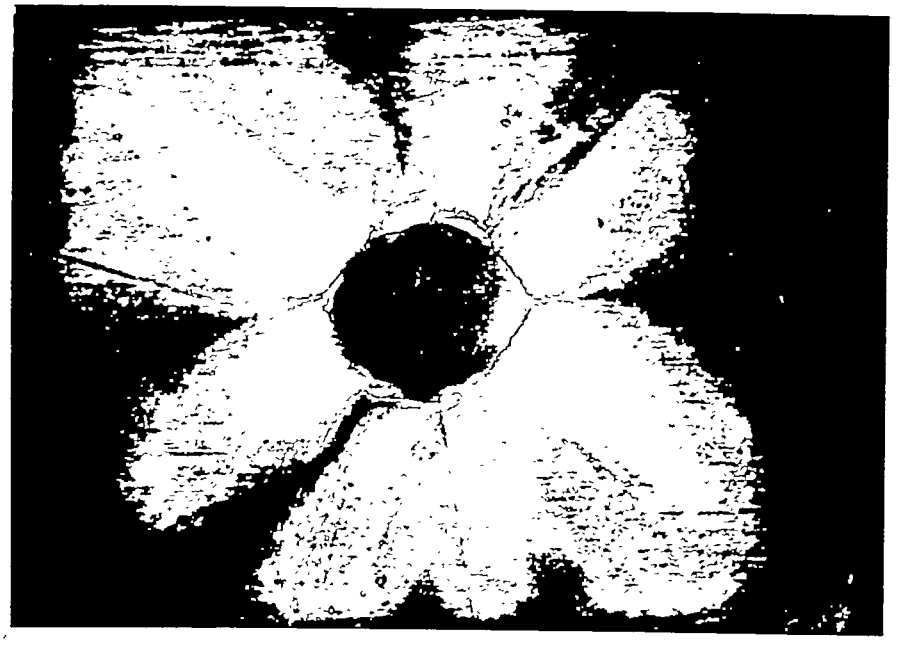

L-81207

(b) 2.6-pound load applied horizontally; Nicols at 10° and 100° to the load; X12.

Figure 17.- Extinction patterns, birefringent banding, and surface lines in specimen N-5.

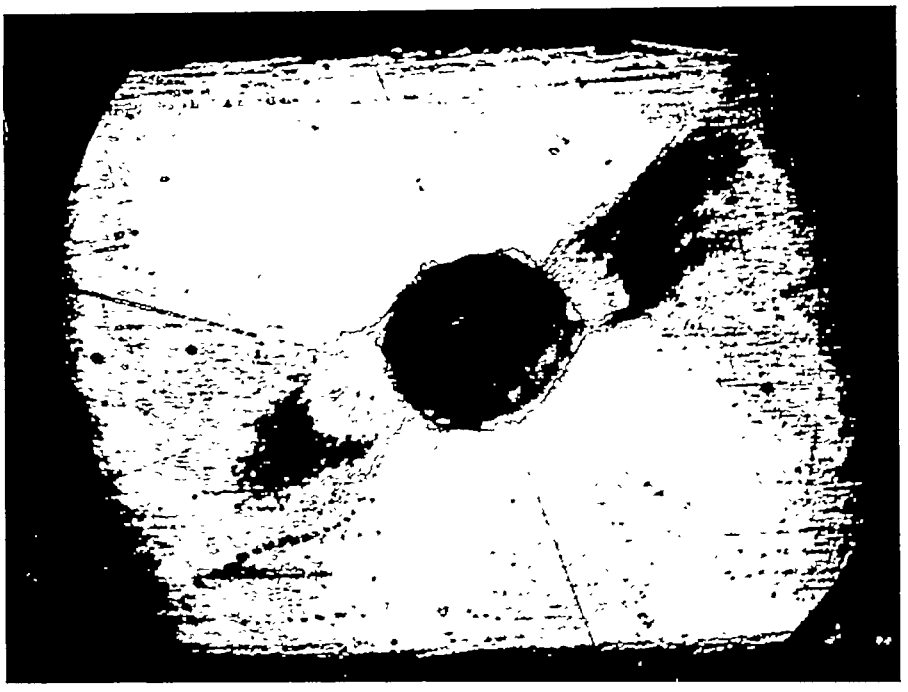

(c) 2.6-pound load applied horizontally; Nicols at 20° and 110° to the load; X12.

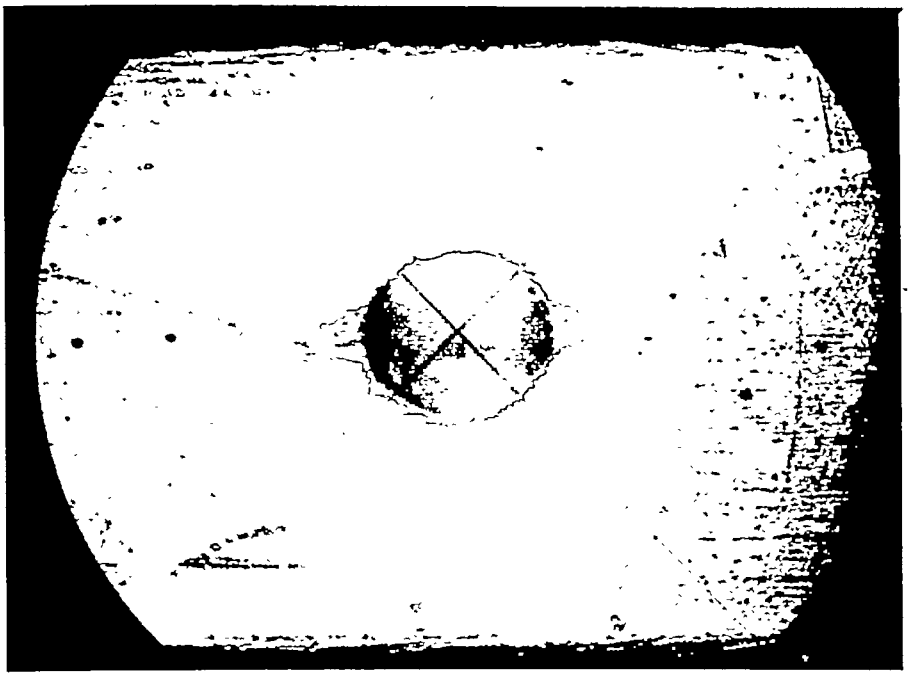

L-81208

(d) 2.6-pound load applied horizontally; Nicols at 45° to the load; X12.

Figure 17.- Continued.

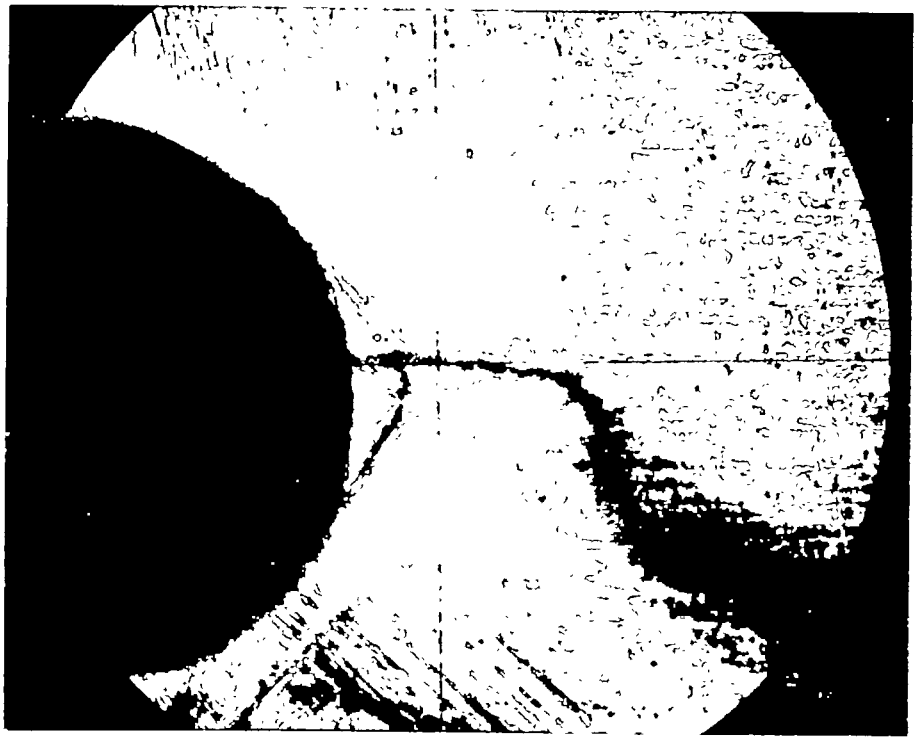

(e) 3.6-pound load applied horizontally; Nicols horizontal and vertical; X42.

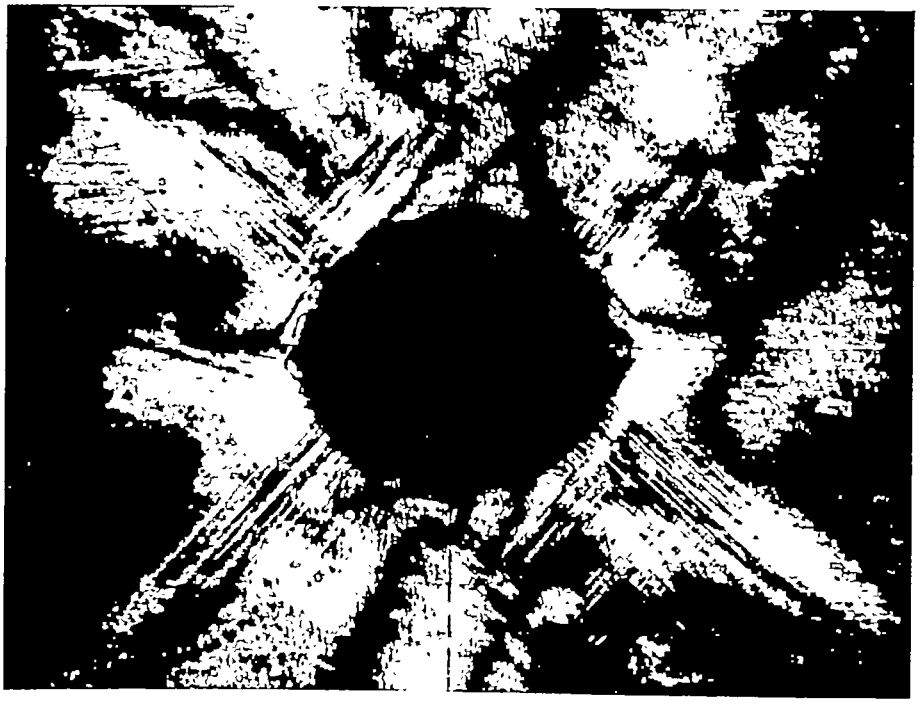

L-81209

(f) Unloaded from 3.6 pounds; Nicols horizontal and vertical; X19.5.

Figure 17.- Concluded.

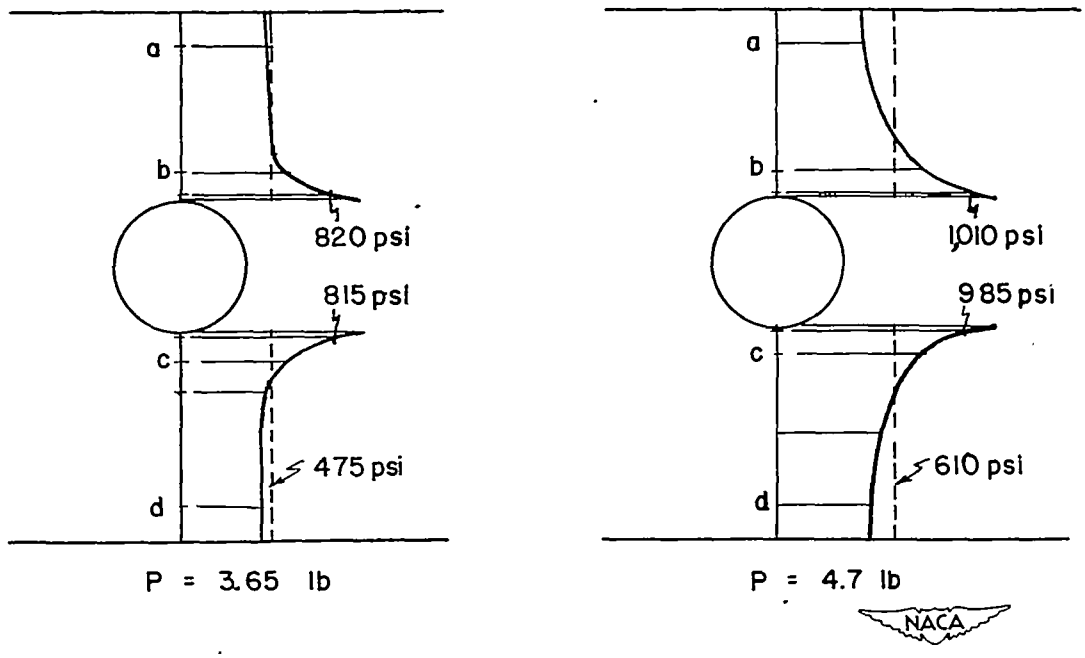

Figure 18.- Variation of stress across minimum section. Specimen N-5.

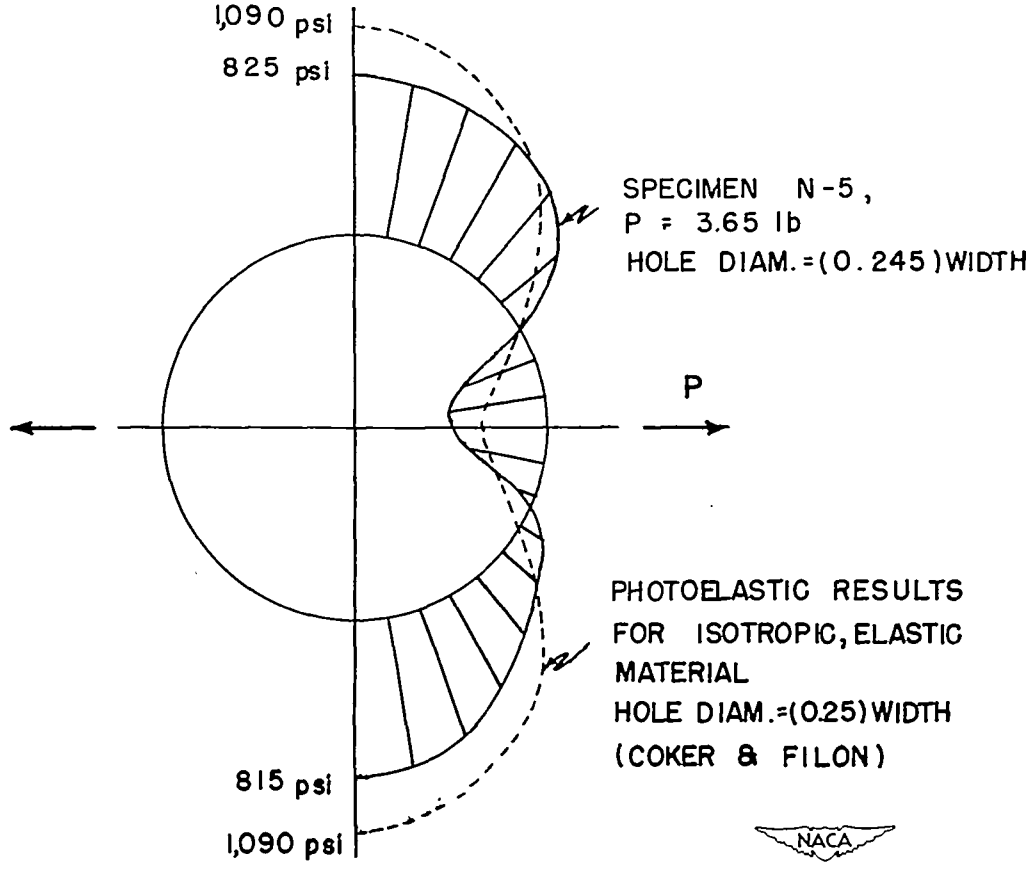

Figure 19.- Variation of stress around rim of hole. Specimen N-5.

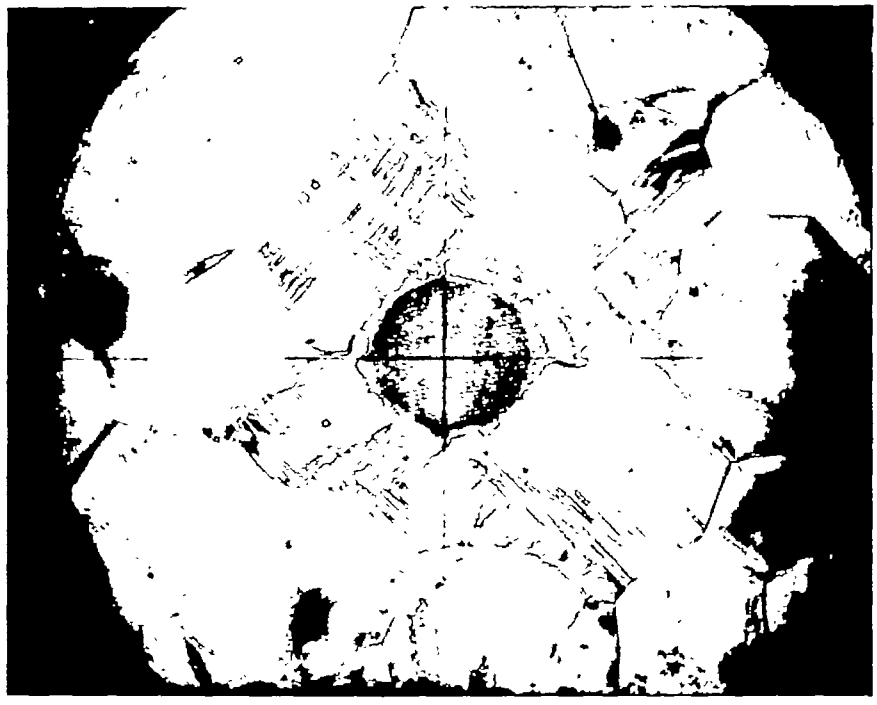

(a) Specimen N-1. Stress, 570 psi.

(b) Specimen N-2. Stress, 565 psi. L-81210

Figure 20.- Surface lines in polycrystalline specimens having a center hole or edge notches. Nicols horizontal and vertical; load applied horizontally; X12.

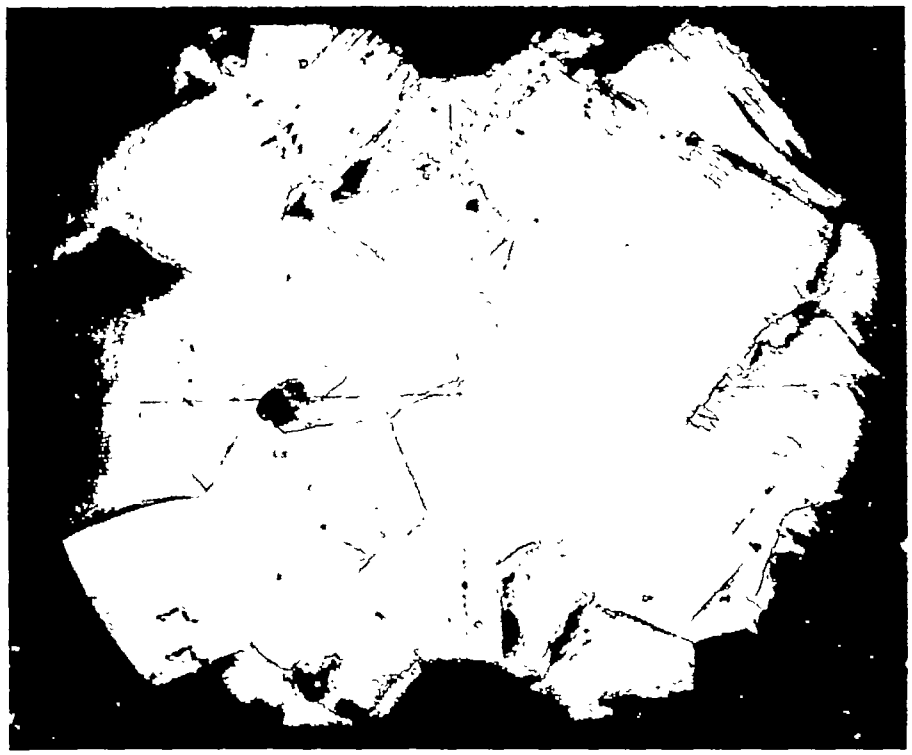

L-81211

(c) Specimen N-3. Stress, 500 psi.

Figure 20.- Concluded.

NACA-Langley - 11-4-53 - 1000